Summary of Professional Accomplishments

I. **Name:** Karolina Anna Mikulska-Rumińska

II. **Diplomas, degrees conferred in specific areas of science:**

2014   **Ph.D. in Biophysics** (*5% in the top ranking of the university*)
Faculty of Physics, Astronomy and Informatics
Nicolaus Copernicus University in Torun, Poland (NCU)
Ph.D. dissertation: *Nanomechanics of neuronal cell adhesion molecules – studies with steered molecular dynamics and single molecule force spectroscopy* (**with honors**)
supervised by Prof. Wieslaw Nowak

2009   **Master's Degree in Physics, spec. Medical Physics**
Faculty of Physics, Astronomy and Informatics NCU
M.Sc. dissertation: *AFM and SMD study of mechanical properties of the cell adhesion protein contactin*
supervised by Prof. Wieslaw Nowak

2007   **Bachelor's Degree in Physics, spec. Medical Physics and Computer Applications**

III. **Information on employment in research institutes or faculties:**

XI 2019 - present   Institute of Physics, Nicolaus Copernicus University in Torun ("adiunkt", *assistant professor*)

I 2016 - VI 2018   School of Medicine, University of Pittsburgh, USA (*postdoctoral associate* in Prof. Ivet Bahar's group)

X 2013 - X 2019   Institute of Physics, Nicolaus Copernicus University in Torun (*research and teaching assistant*)

IX 2013 - III 2014   Laboratory of Physics of Living Matter, École Polytechnique Fédérale de Lausanne (EPFL), Switzerland (*visiting Ph.D. student* in Prof. Giovanni Dietler's group)

IV. **Description of the achievements, set out in art. 219 para 1 point 2 of the Act**

IV.1. Title of the achievement:

Deciphering molecular machinery, physical interactions, signal transduction, and inhibition of the ferroptosis process

The researcher, Dr. Karolina Mikulska-Ruminska (referred to as 'I'), does indicate that the scientific achievement following the Act on Scientific Degrees and Titles consists of a series of publications focused on the studies of the regulated cell death process called ferroptosis.

IV.2. Scientific aims, motivation, description of the results and possible applications

My scientific achievement is focused on the theoretical studies of a newly found form of the programmed/regulated cell death process called ferroptosis. Ferroptosis is characterized by the accumulation of lipid peroxides in the presence of iron, leading to their fatal levels in the lipid membrane which eventually cause a cell death [1]. Although recent research has demonstrated the importance of ferroptosis for human health and its correlation with different kinds of diseases, many aspects of ferroptotic mechanisms are still poorly understood. Notably, activating or blocking ferroptosis alleviates the progression of the disease, providing a promising therapeutic strategy for many diseases [2].

The research presented as the achievement was commenced during my postdoctoral fellowship in the group of Prof. Ivet Bahar in the *School of Medicine* at the *University of Pittsburgh* (Pittsburgh, USA) in collaboration with experimentalists, mainly the group of Prof. Valerian Kagan from the *Graduate School of Public Health* at the *University of Pittsburgh,* and a group of Prof. Hülya Bayır from the *Children's Hospital of Pittsburgh*. The Bahar lab's expertise includes elastic network models, computational and system biology research together with the development of new bioinformatical tools, whereas the collaborators from experimental groups were providing lipidomics experiments, mass spectroscopy measurements, imagining, experiments on cells, and experiments that include animals and patient's samples.

I joined the Bahar Laboratory as a physicist with experience in experimental and computational biophysics and bioinformatics. The collaboration with all groups led us to the first groundbreaking results on ferroptotic mechanisms published in three high-impact factor journals [**H1-H3**]. After my return to the Institute of Physics at the Nicolaus Copernicus University in Torun (Poland), I continued collaborative work on the ferroptosis topic, which resulted in the next significant findings [**H4-H8**]. Further studies were carried out partially in cooperation with yet other groups who provided experimental validation on different aspects of the ferroptosis process.

IV.2.1. Introduction and research motivation

The human body is composed of about 10^{12}-10^{16} cells [3]. All normal cells undergo growth and death, and their lifetime is precisely regulated. Sometimes cell lines gain immortality defined by growth above the Hayflick limit [4], which may lead to cancer [5]. There are two main patterns of cell death: accidental (ACD), when cells are exposed to extreme physicochemical or mechanical stimuli die uncontrollably, and regulated (RCD), being a part of physiologic programs protecting our organisms against incontrollable immortality or being activated upon adaptive responses failure [6]. RCD, essential for normal development [7] or homeostasis [8, 9], is a natural and highly orchestrated process that takes place inside cells. Traditionally, cell death has been divided into only two types: apoptosis and necrosis. However, recent studies have shown that there are more RCD modes, such as pyroptosis (2001), necroptosis (2005), or ferroptosis (2012), that have district morphological and biochemical characteristics [2, 10].

In 2012, the scientific community was moved by the proposed concept of a new iron-dependent and non-apoptotic form of RCD that is characterized by the formation and accumulation of lipid peroxides that are causing massive lipid peroxidation-mediated

membrane damage. This form was named ferroptosis [11, 12]. It was established that ferroptosis is distinct from other RCD programs, and it does not have morphological characteristics of typical necrosis or apoptosis [10, 11]. In fact, ferroptosis occurs in cells as reduced mitochondrial volume, reduced or disappearance of mitochondrial cristae, and increased outer mitochondrial membrane rapture [10, 11]. Mitochondria are the cell's powerhouses, and they host cellular respiration, one of the most important processes in organisms. Therefore, ferroptosis have a critical impact on diseases in the nervous system, heart, lungs, liver, or kidney (**Fig. 1**). Moreover, it has been shown that ferroptosis is correlated with neurodegenerative diseases, e.g., in Alzheimer's [13, 14], Parkinson's [15, 16], or Huntington's [17] where the observed levels of iron-dependent lipid peroxides are elevated, as well as in cerebello-cortical atrophy, sepsis, bacterial and viral diseases [18]. Controlled induction of ferroptosis has potential in cancer therapy and immunity [19-22]. Ferroptosis might be an essential cause of multiple organ inflammation in COVID-19 [23-26], and can contribute to the degradation of tissue, as it happens in kidney failure, brain trauma, and asthma [27-29].
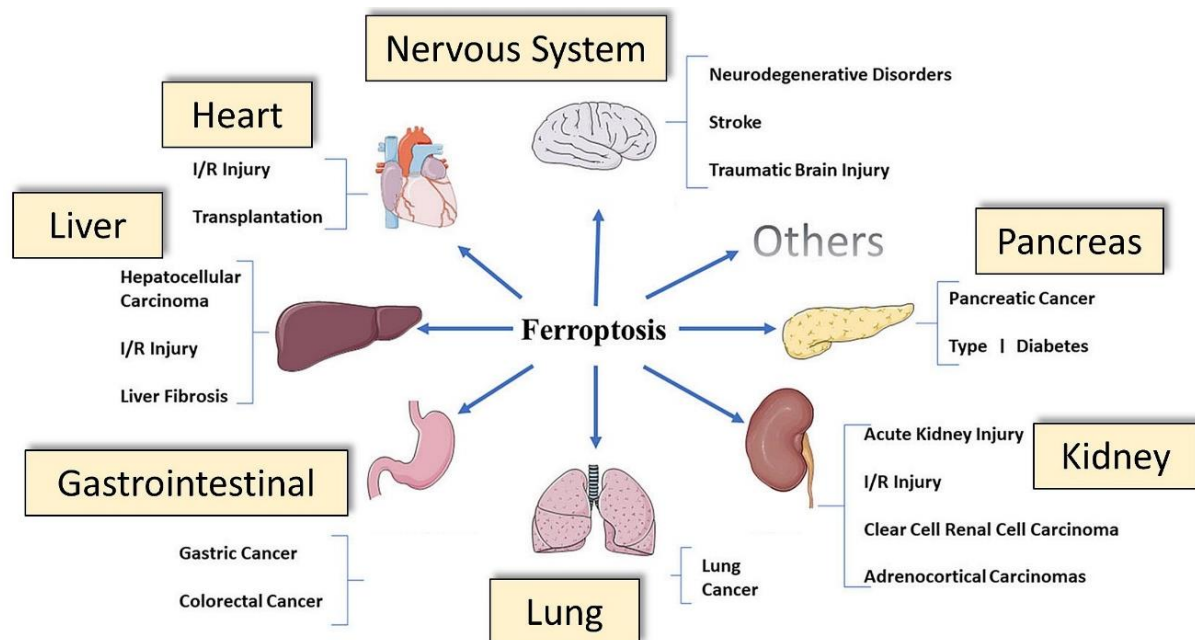

Figure 1. The role of ferroptosis in a variety of system diseases. Modified source figure [2].

Before presenting the methods of theoretical molecular biophysics employed to study the mechanisms involved in the ferroptosis process, I need to introduce key biochemical concepts for better understanding of my habilitation achievements.

Ferroptosis involves various biological pathways. It can be triggered by the loss of the control of one over three major processes: iron metabolism (**Fig. 2a**, *black dashed line*), lipid peroxidation (**Fig. 2b**, *blue dashed line*) or thiol regulation (**Fig. 2c**, *red dashed line*). Iron-dependent lipid peroxidation is the main trigger for the activation of ferroptosis [28]. Since a similar iron-driven catalytic scheme applies in more than one process, the hypotheses on the types of iron-driven peroxidation processes vary from strictly enzymatic to non-enzymatic [30]. The non-enzymatic oxidation process occurs via the Fenton reaction (*Iron Metabolic Pathway*), whereas the candidates for the enzymatic oxidation of polyunsaturated fatty acids (PUFAs) are proteins called lipoxygenases (LOXs) [31]. PUFAs are essential components of biological

membranes and regulate inflammation, immunity, cell growth, or synaptic plasticity [32, 33]. PUFAs are substrates of peroxidation during the ferroptosis process due to the presence of a weak C–H bond at the bis-allylic positions (*green circle* in **Fig. 4**) [34]. PUFAs vary in the number of double bonds, and a higher number of double bonds in PUFA increases its susceptibility to oxidation [35]. Moreover, newly oxidized molecules can oxidize other PUFAs [36]. To set my research in a proper perspective, three major metabolic pathways shown in **Fig. 2**, are further described.
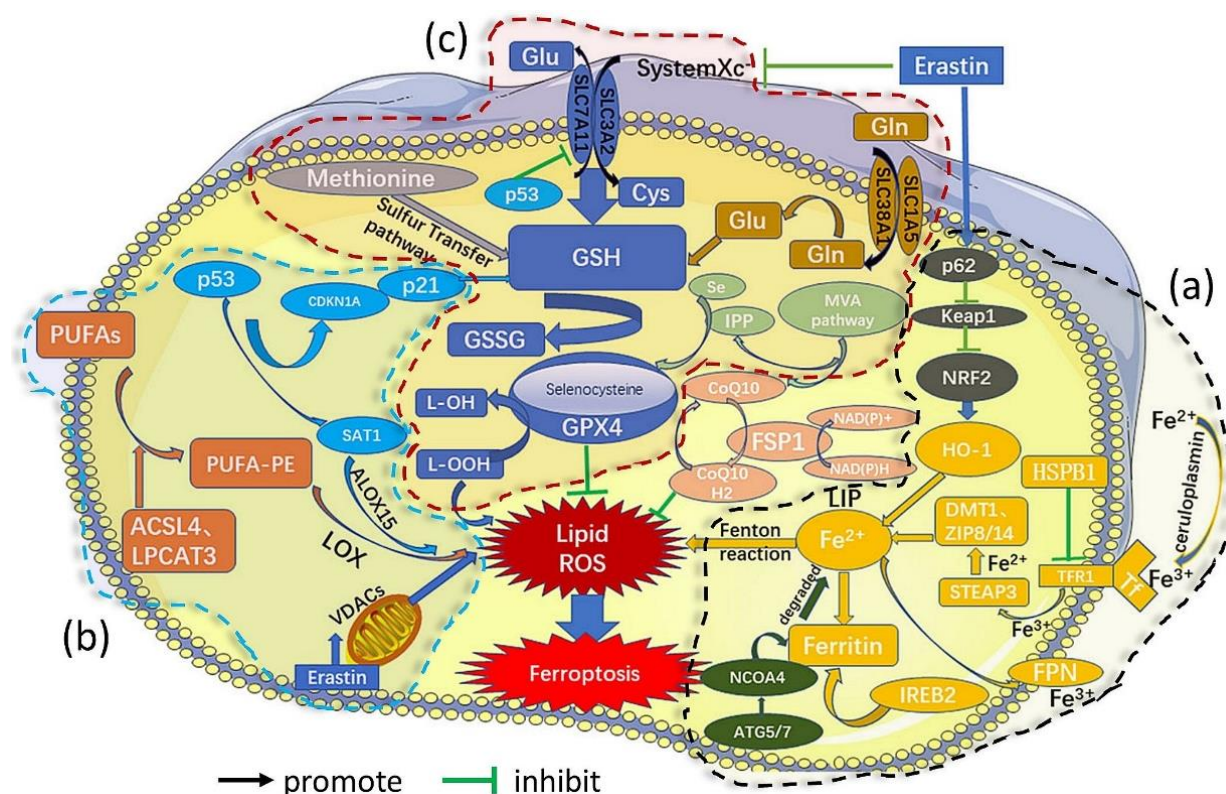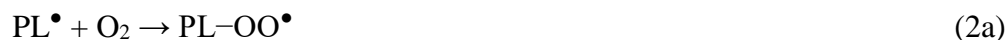

Figure 2. Overview of ferroptosis modulation and contribution from three main metabolic pathways. *(a) Iron Metabolic Pathway, (b) Lipid Oxidation Metabolic Pathway, and (c) Glutathione Metabolic Pathway. Modified figure from* [2]*.*

Iron Metabolic Pathway. In the human body, iron metabolism is strictly controlled at the cellular and systemic levels using an adjusted balance between proteins to provide the precise amounts of iron needed for biological functions [37, 38]. Iron might accept and donate electrons, therefore, it can be found in an organism in ferrous (Fe^{2+}) and ferric (Fe^{3+}) forms. In the mitochondria, the O_2-dependent oxidation of carbs fuels gives rise to reduced oxygen species, i.e., ROS, which are important signaling molecules. However, ROS becomes toxic at higher concentrations [39]. Iron may directly generate excessive ROS through the Fenton reaction [40], thereby increasing oxidative damage and leading to lipid peroxidation, membrane damage, and cell death [11]. In non-enzymatic lipid peroxidation, which refers to the Fenton reaction, Fe^{2+} is oxidized to Fe^{3+} through a reaction with hydrogen peroxide (H_2O_2), resulting in the formation of highly reactive hydroxyl radicals ($OH^\bullet$) (**Fig. 3**). Fe^{3+} is further reduced back to Fe^{2+} through reaction with superoxide radicals ($O_2^{\bullet-}$), and hydroxyl radicals ($OH^\bullet$) abstract hydrogen from PUFA forming a carbon-centered phospholipid (PL) radical ($PL^\bullet$) as follows:

$$PL-H + R^\bullet \rightarrow PL^\bullet + R-H \qquad\qquad (1)$$
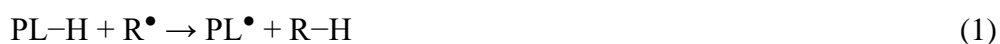
Then, phospholipid radical PL$^{\bullet}$ can react with molecular oxygen (O_2), forming a phospholipid peroxyl radical (PL−OO$^{\bullet}$) which further abstracts hydrogen from another PUFA, creating a phospholipid hydroperoxide (PL−OOH) and a new PL$^{\bullet}$, which can consecutively react again with another O_2. This drives the formation of the next PL−OO$^{\bullet}$ and propagates the radical process to adjacent lipid molecules.

$$PL^{\bullet} + O_2 \rightarrow PL-OO^{\bullet} \tag{2a}$$

$$PL-OO^{\bullet} + PL-H \rightarrow PL^{\bullet} + PL-OOH \tag{2b}$$

$$PL-OOH + Fe^{2+} \rightarrow PL-O^{\bullet} + OH^- + Fe^{3+} \tag{2c}$$

The last step of peroxidation is termination, where numerous enough radical species spontaneously react to yield non-radical breakdown products [39]. Moreover, PL−OOH may decompose to 4-hydroxynonenal (4-HNE) or malondialdehyde (MDA) (**Fig. 3**), which by crosslinking, may inactivate proteins [41]. The peroxidation process and generation of 4-HNE or MDA lead to membrane instability and permeabilization and finally to the cell death.
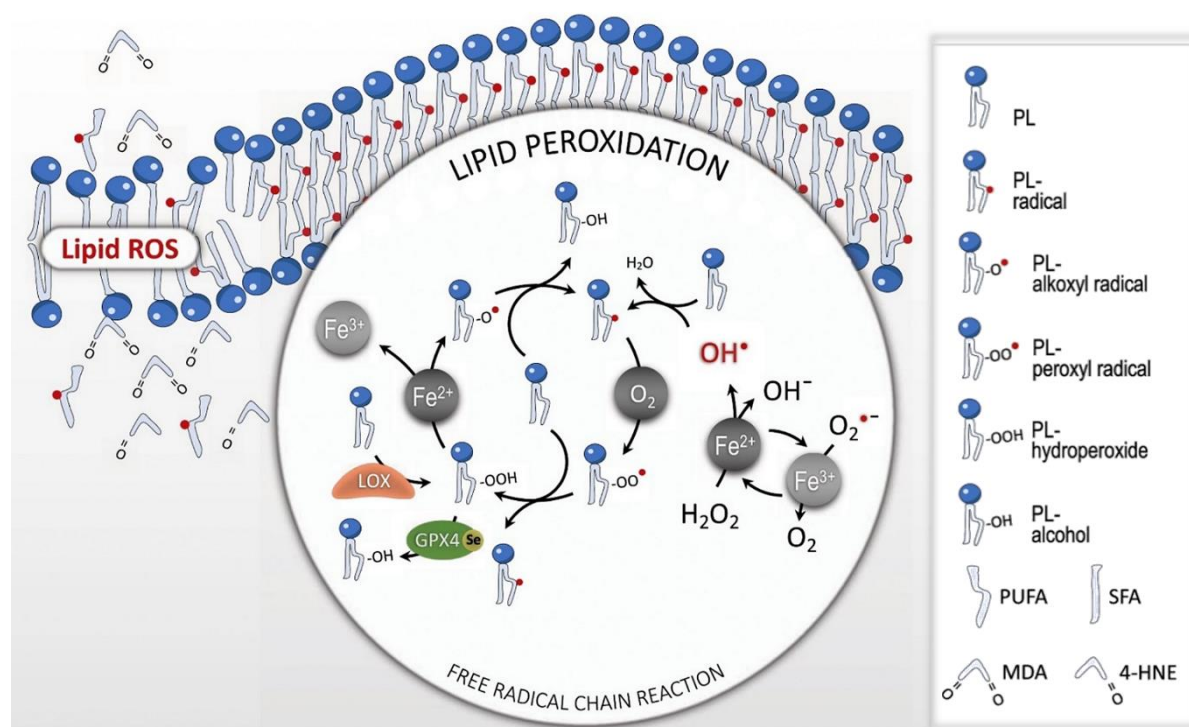
$$PL-OO^{\bullet} + PL-OO^{\bullet} \rightarrow Nonradical\ breakdown\ products \tag{3}$$

Figure 3. Non-enzymatic and enzymatic lipid peroxidation process. *The non-enzymatic lipid peroxidation process includes the Fenton reaction, i.e., Fe^{2+} is oxidized to Fe^{3+} through a reaction with H_2O_2 and generates highly reactive OH$^{\bullet}$ radicals. Enzymatic lipid peroxidation includes here: (i) lipoxygenase (LOX), which generates lipid hydroperoxides, and (ii) glutathione peroxidases 4 (GPX4), which reduces reactive lipid hydroperoxides into unreactive lipid alcohols, which interrupts the free radical chain reaction and suppresses further lipid peroxidation. Figure adopted from [41].*

Before the Fenton reaction could occur, a few other required pathways should be executed and work in a certain way (**Fig. 2**, *black dashed shape*). The iron metabolic pathway starts when Fe^{3+} enters through the membrane protein transferrin receptor 1 (TFR1), and it is converted to Fe^{2+} iron by iron reductase. The unstable Fe^{2+} is then released into the labile iron pool (LIP) in

the cytoplasm by the divalent metal transporter 1 (DMT1). Here, the six-transmembrane epithelial antigen of prostate 3 metalloreductase (STEAP3) reduces Fe^{3+} enabling DMT1 to export iron. Excess iron ions can be stored in ferritin in the form of Fe^{3+} or remain labile by being released via the membrane protein ferroportin (FNP) to maintain the labile iron pool at a low level to avoid cell toxicity [38, 42]. HSPB1 acts as a negative regulator of ferroptosis, reducing the uptake of iron and lipid peroxidation [43]. Several other factors can additionally impact the main iron regulatory pathway, e.g., the nuclear factor (erythroid-derived 2)-like 2 (NRF2) transcription factor, which is a modulator of iron signaling [44] or nuclear receptor co-activator (NCOA)4 that mediates autophagic ferritin degradation [45].

Lipid Oxidation Metabolic Pathway. Iron is used for the synthesis of metalloproteins, such as hemoglobin (oxygen transport) or cytochromes (electron carriers), to form organic (e.g., heme group) or inorganic (e.g., Fe/S clusters) cofactors [10]. Since ferric iron is poorly soluble at neutral pH [46], the organisms have developed means to absorb iron in a complex with proteins which are called non-heme proteins [47], e.g., transferrins (use to traffic and import non-heme iron) [48] or lipoxygenases [49] (catalyze the dioxygenation of PUFAs and generate PL−OOH, ferroptotic cell death signal). Lipoxygenases are the main object of this study, and belongs to the enzymatic aspect of ferroptosis.

Lipoxygenases (LOXs) are non-heme iron-containing enzymes that can catalyze the oxygenation of free [50] (e.g., arachidonic acid, AA) or esterified PUFAs [**H1**] [PUFA-PLs; e.g., phosphatidylethanolamine (SA-PE) or cardiolipin (CL)] [10] to generate various lipid hydroperoxides, i.e., PUFAs with insertion of O_2 into C-H bond flanked in two isolated cis-double bonds in the oxidizable PUFAs tail (*green circle*, **Fig. 4**).
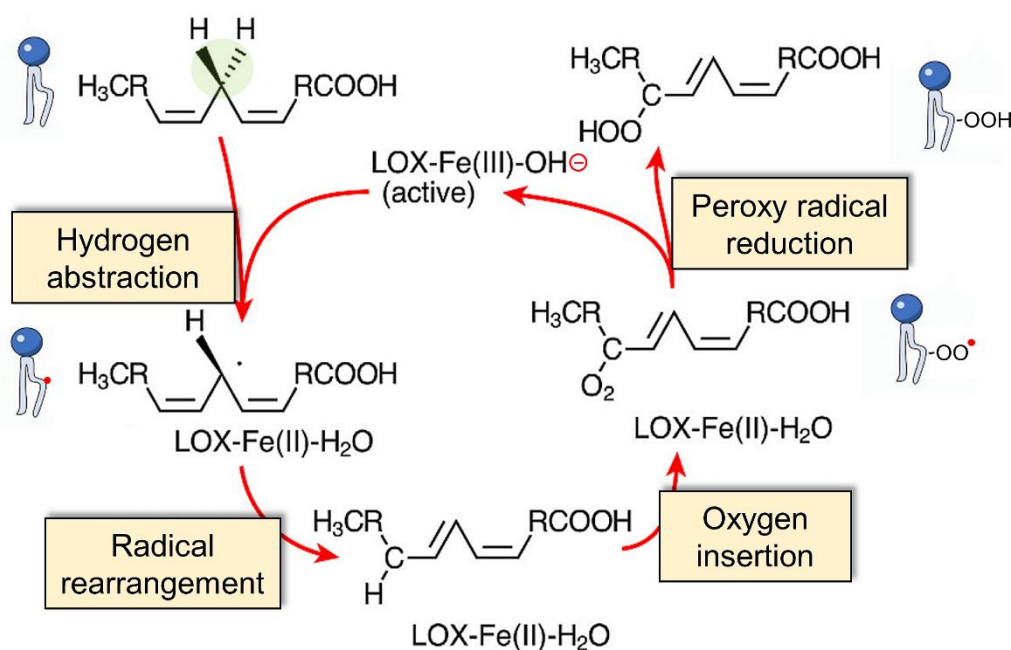

Figure 4. A schematic diagram of LOXs catalytic reaction cycle*. Most of the LOXs catalyze the insertion of molecular oxygen into PUFA, leading to the formation of corresponding lipid hydroperoxides in four steps: (1) hydrogen abstraction, (2) radical rearrangement to another carbon center, (3) oxygen insertion to the rearranged carbon radical center, and (4) peroxy radical reduction. Modified figure adopted from* [51].

The catalytic reaction is similar among LOXs and includes four steps (**Fig. 4**):

(i)   hydrogen abstraction from bisallylic methylene carbon of PUFA by the $Fe(III)-OH^-$ cofactor, yielding $Fe(II)-OH_2$ and formation of a fatty acid radical ($PL^\bullet$),

(ii)   radical rearrangement to another carbon center,

(iii)   molecular oxygen (O_2) insertion to the rearranged carbon radical, thereby forming a phospholipid peroxy radical ($PL-OO^\bullet$) bonded to the rearranged carbon, and

(iv)   reduction of the peroxy radical to its corresponding anion ($PL-OOH$) [51-53]. Such products can cause damage to the lipid bilayer of the membrane [49].

One should note that cellular lipids include thousands of lipid species that vary in quantity, distribution, and functions. In fact, the higher concentration of PUFAs in the cell, the more significant damage might be caused by the lipid peroxidation process and the extent of ferroptosis, which can vary among diseases and organs/tissues [49]. Free PUFAs are the substrates in these reactions. However, in some cases, such as phosphatidyl ethanolamine (PE), first must be esterified with membrane phospholipids to be further oxidized to transmit the ferroptotic signal [2]. This process involves two proteins, acyl-CoA synthetase long-chain family member 4 (ACSL4) and lysophosphatidylcholine acyltransferase 3 (LPCAT3), which participate in the biosynthesis and remodeling of PUFAs in the esterification reactions [49] (**Fig. 2b**, *blue dashed line*). Esterified PUFAs-PE can be further oxidized by LOXs, which involve molecular oxygen binding on an iron center and conversion of molecular oxygen into an active species to induce ferroptosis in cells [54]. Lipid peroxidation of PUFAs generates different oxidation products, and some of them are highly cytotoxic and pathogenic [10].

The mammalian LOX family is coded by six known functional genes [12, 36, 51] which are termed arachidonic acid lipoxygenase (ALOX). There are six human isoforms of LOXs (E3-LOX, 5-LOX, 12-LOX-1, 12-LOX-2, 15-LOX-1, 15-LOX-2) that are categorized with respect to their positional specificity of PUFAs oxygenation [55]. The digit indicates the number of the carbon atom of sn-2 chain of PUFA at which molecular oxygen will be most often inserted.

It is worth mentioning that the P53-SAT1-ALOX15 pathway is also involved in the regulation of ferroptosis [56]. SAT1 (spermidine/spermine N1-acetyl transferase 1) is an enzyme and a transcriptional target of P53, which induction is correlated with the expression levels of 15LOX, and SAT1-induction of ferroptosis is significantly abrogated in the presence of a 15LOX inhibitor [2, 56].

Glutathione Metabolic Pathway. Cells have several escape mechanisms against cell death [57, 58]. In ferroptosis, such mechanism includes a protein called glutathione peroxidases 4 (GPX4) which plays an indispensable role in the regulation of ferroptosis by reducing toxic lipid hydroperoxides ($PL-OOH$) to non-toxic lipid alcohols ($PL-OH$), thereby limiting the propagation of lipid peroxidation within the membrane (**Fig. 5**) [39, 59, 60]. In humans, several GPXs (GPX1-8) vary in function, cell localization, and substrate specificity [61, 62]. Compared to other GPX enzymes, GPX4 is unique in its ability to reduce large organic peroxides, including polyunsaturated lipids and sterols [39], thus preventing the accumulation of lipid ROS [11, 28]. GPX4 uses glutathione (tripeptide composed of three residues glutamic acid, cysteine, and glycine), the most abundant thiol in animal cells [63], as a cofactor. Glutathione exists in reduced (GSH) and oxidized (GSSG) states and is catalyzed by GPX4 in the following reaction:

$$2\,GSH + PL-OOH \rightarrow GSSG + PL-OH + H_2O \tag{4}$$

This reaction occurs in the GPX4 active site, which is formed by selenocysteine, glutamine, and tryptophan (catalytic triad) and shuttles between oxidized and reduced states. The catalytic cycle of GPX4 starts when the active selenol (Se−H) is oxidized by peroxides substrate to selenic acid (Se−OH). Then, the first GSH molecule is used to reduce to an intermediate selenodisulfide (Se−SG) which is further reduced by the second GSH molecule, releasing the GSSG molecule [36, 39] (**Fig. 5**). GSSG can be regenerated to GSH form by the enzyme glutathione reductase [22, 64] which utilizes NADPH as the source of the electron [65].
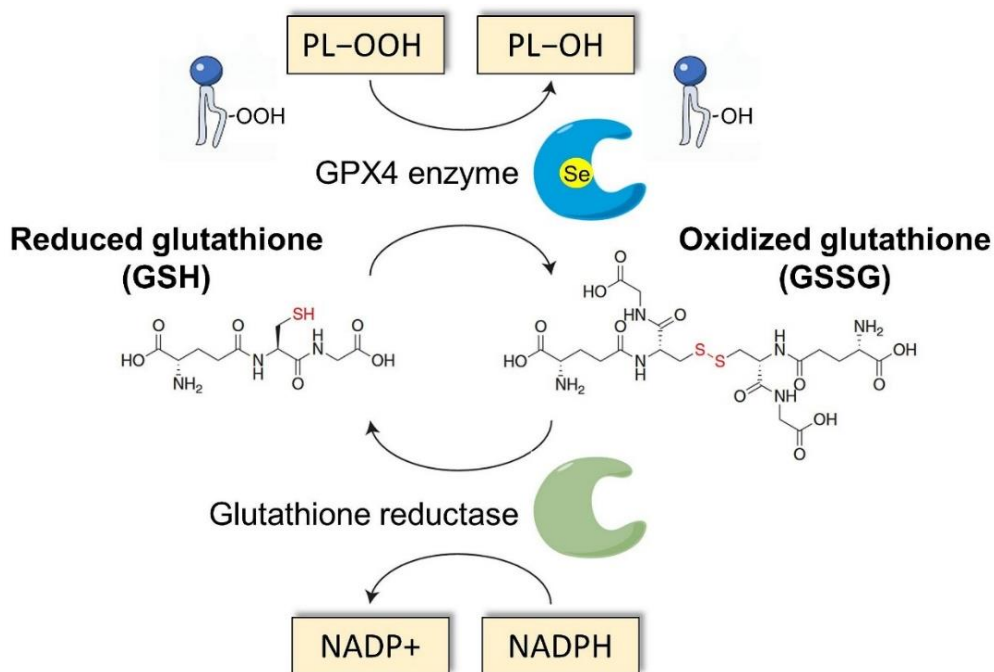

Figure 5. GPX4 enzymatic reaction. *Modified figure adopted from* [39].

The influence of the glutathione generation has extracellular cystine, which is exchanged for intracellular glutamate in a 1:1 ratio by the plasma membrane cystine/glutamate antiporter (System Xc⁻, **Fig. 2**) and then converted to cysteine, which is required to generate GSH. Suppression of cysteine uptake leads to the accumulation of lipid peroxidation products [66]. In healthy cells, more than 90% of the total glutathione pool is in the reduced form (GSH) [67], and the ratio of GSSG to GSH suggests the level of cellular oxidative stress [68]. Due to GPX4's prominent role in catalyzing the reduction of lipid peroxides in a glutathione-dependent reaction, it is called a key regulator of ferroptosis.

Additional ferroptosis pathways and regulators. Recent years have brought a dynamic increase of interest in the ferroptosis process [69] which can be seen by the number of scientific articles that are published each year (**Fig. 6**). Since the discovery of ferroptosis in 2012 by the *Stockwell's group* till November of 2022, a total number of 5031 publications were collected by searching for "ferroptosis" in abstracts in the *Web of Science*. The effort of scientists who are elaborating on ferroptosis shed light on new regulators and the involvement of other metabolic pathways correlated with this process, and some of them will be described in this paragraph.
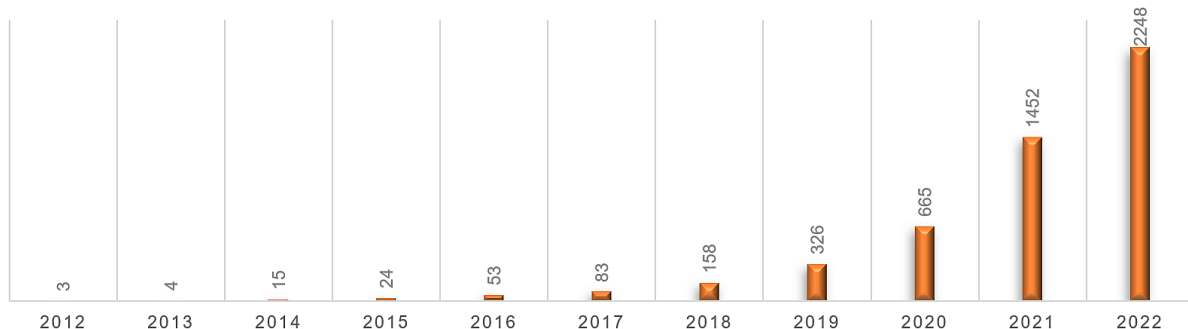
Figure 6. Annual frequency of publications in the field of ferroptosis. Plot generated based on the information provided by the Web of Science database (from 22 IX 2022).

CoQ Metabolic Pathway. Except for the three major metabolic pathways described above, scientists are still finding new relations between ferroptosis and other components of the cellular system. It was recently established that glutathione-independent ferroptosis could be stopped by the recently identified ferroptosis suppressor protein 1 (FSP1) [70, 71]. FSP1 contains an N-myristoylatated residue (lipidic modification) which mediates the recruitment to the plasma membrane and a flavoprotein oxidoreductase domain required for suppressing ferroptosis. Upon recruited to the plasma membrane-enriched organelles, FSP1 reduces coenzyme Q_{10} (CoQ_{10}) to ubiquinol ($CoQ10\text{-}H_2$, **Fig. 2**), which further blocks lipid peroxidation by acting as a lipid peroxyl radical trap [1, 70]. CoQ_{10} is a mobile lipophilic electron carrier that synthesizes lipid-soluble antioxidants [72]. However, CoQ_{10} alone is not sufficient to stop the propagation of lipid peroxides unless it is kept reduced as $CoQ_{10}\text{-}H_2$, and then it can be used in the following way [73]:

$$CoQ_{10}\text{-}H_2 + PL{-}OO^\bullet \rightarrow CoQ_{10}^{\bullet-} + H^+ + PL{-}OOH \tag{5}$$
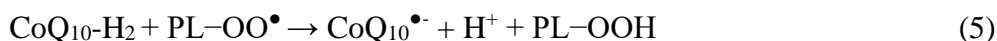
The product of this reaction, the ubisemiquinone-10 radical, $Q_{10}^{\bullet-}$, might further scavenge another radical as follows:

$$CoQ_{10}^{\bullet-} + H^+ + PL{-}OO^\bullet \rightarrow CoQ_{10} + PL{-}OOH \tag{6a}$$

$$2\,CoQ_{10}^{\bullet-} + 2\,H^+ \rightarrow CoQ_{10}\text{-}H_2 + Q_{10} \tag{6b}$$

FSP1 can also directly reduce oxidized CoQ_{10} to the reduced state by using NADH as a cofactor [70]. It was suggested by *Bersuker et al.* that the FSP1 protection branch might be secondary to GPX4, occasionally becoming primary in certain conditions [1].

Nitric oxide synthase. Inducible isoform of nitric oxide synthase (iNOS) generates NO [13], whose reactivity towards different radical intermediates of lipid peroxidation was discovered over 30 years ago [14]. We have shown that NO inhibits lipid peroxidation generated by lipoxygenase complex with another protein called PEBP1 [**H5-H6**]. A description of this finding will be explained in the **Results** paragraph.

Phospholipase iPLA₂β. Our recent studies also showed that Ca^{2+}-independent phospholipase $A_2\beta$ ($iPLA_2\beta$) could hydrolyze peroxidized phospholipids that are generated by lipoxygenases and, therefore, can eliminate the ferroptotic cell death signal [**H8**]. A description of this finding will be provided in the **Results** paragraph.

IV.3.2. Methods used to obtain the achievement

Different types of computational biophysical approaches [74] and bioinformatics tools [75] were used during this research study to simulate the physical interactions and dynamics of biological systems involved in the ferroptosis process. The computational results were verified by experimental studies provided by the US collaborators, mainly by Prof. Valerian Kagan and Prof. Hülya Bayır groups from the University of Pittsburgh. The descriptions of the experimental techniques provided by the collaborators will not be included in this application, only the candidate's most commonly used computational methods, briefly described below.

Molecular Docking. Molecular docking [76-79] is a method that allows predicting a preferred orientation of one molecule (*ligand*: protein or chemical compound) vs. another (*receptor*: protein) based on the well-established scoring functions, which evaluate the physical interactions to obtain the highest binding affinity, in order to predict a stable complex [76, 77]. Both approaches, i.e., protein-protein docking and protein-ligand docking, were applied to predict the structure of several complexes that were used in the achievement, including 15LOX-1/PEBP1 and 15LOX-2/PEBP1 protein complexes [**H1**] as well as the initial position of the substrates (PUFAs and PL-PUFAs) [**H2**, **H6**] and the most common ferroptosis inhibitor, ferrostatin-1 [**H7**]. PEBP1/15LOXs models (15LOX-1 and 15LOX-2) with/without substrates were studied by our team very extensively, using both experimental and computational approaches, and several essential observations were addressed therein [**H4-H7**].

Molecular Dynamics (MD) simulations. All-atom classical MD is a standard method that has been used since the late 1970s [80, 81] in biophysics and biochemistry for analysis of the physical movements of atoms and assemblies of molecules [82, 83]. MD involves the iterative numerical calculation of instantaneous forces present in a biomolecular system, causing movement of atoms in response to their molecular interactions according to the classical Newton's equations of motion (eq. 7) which describes the acceleration of atom *i* of mass m_i along a coordinate r_i in time *t*.

$$\vec{F_i} = m_i \frac{d^2 \vec{r_i}(t)}{dt^2}, \qquad i = 1, 2, \dots, N \tag{7}$$

MD simulations are based on knowledge of the energy of the system as a function of the atomic coordinates, which are provided by techniques such as NMR, X-ray, or cryo-EM. Such coordinates are deposited and freely available in the *Protein Data Bank* (PDB) [84] and can be downloaded as PDB files. The general approach is to estimate the forces acting on each atom, which are related to the gradient of potential *V* with respect to the atom positions *r* (eq. 8) and can be used to calculate evolution of the system as a function of time.

$$\vec{F_i} = -\vec{\nabla}_{r_i} V(\vec{r}_1, \dots, \vec{r}_N) \tag{8}$$

The energy functions contain many parametrized terms obtained for the past 50 years from experimental and/or quantum mechanical studies. The constant improvements have finally resulted in the set of functions and associated parameters applied to larger biological structures and termed as a force field. Various force fields, e.g., CHARMM, GROMACS, OPLS, AMBER, have been developed for MD simulation of proteins. Despite the differences, they are all composed of the bonded and the non-bonded terms (**Fig. 7**). Bonded terms describe bonds,

angles, and dihedral interactions within the protein structure, whereas the non-bonded terms state for distant interactions such as electrostatic and van der Waals interactions.

$$E_{total} = \sum_{bonds} K_r(r - r_{eq})^2 + \sum_{angles} K_\theta(\theta - \theta_{eq})^2 + \sum_{dihedrals} \frac{V_n}{2}[1 + \cos(n\phi - \gamma)] + \sum_{i<j} \left[\frac{A_{ij}}{R_{ij}^{12}} - \frac{B_{ij}}{R_{ij}^{6}} + \frac{q_i q_j}{\epsilon R_{ij}} \right]$$

Figure 7. The classical force field in MD simulations. *Modified figure adopted from* [85].

In order to obtain the time evolution of positions *r* and velocities *v* of each atom in the simulated system, numerical methods are employed. The most commonly used is the Verlet algorithm [86], which meets all the requirements imposed on the numerical scheme for solving the equations of motion – it is numerically efficient, stable, and accurate.

$$\vec{r}(t + \Delta t) = \vec{r}(t) + \vec{v}(t)\Delta t + \frac{1}{2}\vec{a}(t)\Delta t^2 \tag{9}$$

$$\vec{v}(t + \Delta t) = \vec{v}(t) + \frac{1}{2}\Delta t[\vec{a}(t) + \vec{a}(t + \Delta t)] \tag{10}$$

$$\vec{a}(t) = -\frac{1}{m}\nabla V(\vec{r}(t)) \tag{11}$$

$\vec{r}$ – atom position, t – time, Δt – time step, $\vec{v}$ – velocity, $\vec{a}$ – acceleration

Moreover, the initial velocities are usually assigned randomly based on the Maxwell-Boltzmann distribution for a given temperature. The relation between temperature and velocities of atoms in the system is described through the equation (12) for kinetic energy and the principle of equipartition of (kinetic) energy:

$$\frac{1}{2}\sum_{i=1}^{N} m_i v_i^2 = \frac{3}{2}Nk_B T \tag{12}$$

k_B – Boltzmann's constant, N – number of atoms, T – temperature,
m_i – a mass of the i-th atom, v_i – velocity of the i-th atom.

Having determined structures and characterized a physical system in terms of model parameters, MD simulations are successfully used to provide a hint for further investigations to experimentalists providing potential explanations of the phenomena that appear at the molecular level.

MD simulations are effectively used by the scientific community for cases when biological systems contain standard elements. The difficulty appears when it comes to the non-standard elements, especially when they are an integral part of the biological system, e.g., the metal ion in the catalytic site (lipoxygenases). In such cases, advanced parametrization knowledge and

quantum calculations (Gaussian B3LYP/6-31(d,p)), which provide information about the geometry and partial charges, are required. We successfully used MD simulations to explain the dynamics and physical interactions of different components of biological systems involved in the ferroptosis process [**H4-H8**], and some of them required parametrization of the catalytic site with a metal ion (e.g., 15LOX-1 [**H4**], 15LOX-2 [**H5-H7**]), or non-standard molecules, e.g., ferrostatin-1 [**H7**] or lipid peroxides [**H8**]. More detailed information about classical MD can be found in the following articles [83, 87, 88].

Elastic Network Models (ENMs). ENMs are classified as entropic models, which in the past years demonstrated in many studies their abilities to successfully capture the long-term dynamics of biological systems, providing experimental verifications of the predicted outcome [89-91]. ENMs use simplified uniform harmonic potentials for the interacting components of protein structure. We are considering residues represented by their C^α atoms for protein structures. In ENMs, we can distinguish two types of modes: low- and high-frequency modes, which provide a simple and interpretable description of the protein's collective motion. It has been shown that low-frequency normal modes correspond to the cooperative motions of large parts of the protein structure, which are essential for protein function, and their long-range character enables allosteric interaction of various parts of the protein structure that are spatially distant from one another [92-94].

There are two simple yet powerful ENMs models for predicting collective dynamics of protein structure that are giving good correspondence to the experimental observations: the Gaussian Network Model (GNM) introduced by Prof. Ivet Bahar (former PI of the candidate) and coworkers [95], and its extension to three dimensions described as Anisotropic Network Model (ANM) [96]. GNM network is composed of beads/nodes whose position R_k is represented by C^α atom for each residue from protein structure (**Fig. 8A**). Springs connect residues located within a cutoff r_c distance (e.g., 10 Å). For two nodes i and j, there are equilibrium position vectors, R_i^0 and R_j^0, from which we can obtain equilibrium distance vector R_{ij}^0 (**Fig. 8B**). Nodes and inter-residue distances R_{ij} undergo Gaussian fluctuations, which are defined ΔR_i for node i and ΔR_j for node j, thus instantaneous fluctuation vector between nodes i and j is expressed as follows: $\Delta R_{ij} = \Delta R_j - \Delta R_i$.
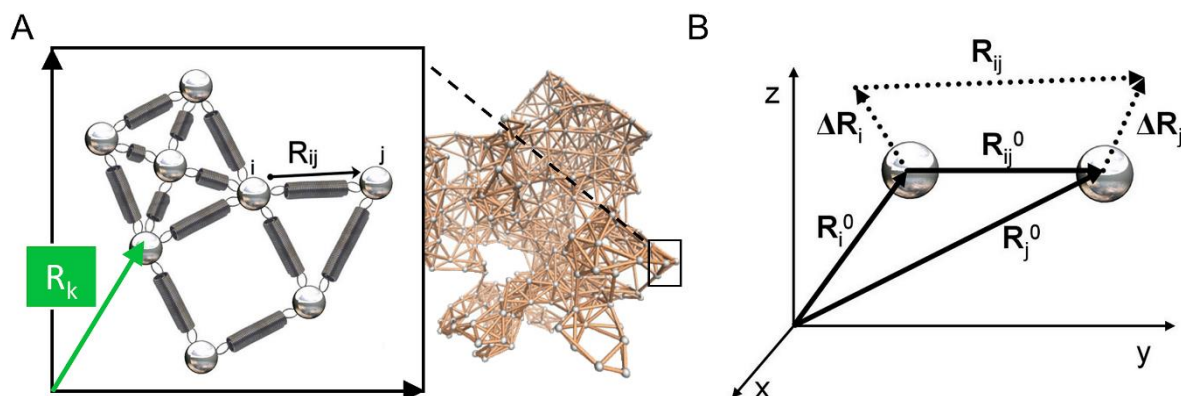

Figure 8. Concept of the Gaussian Network Model. *(A) Representation of protein structure with beads corresponding to C^α atoms and springs connecting beads within cutoff distance. (B) Schematic representation of two beads/nodes, i and j, in GNM concept. Modified from Wikipedia.*

The potential energy of the network is defined based on the theory of elasticity of Flory [97] and the Rouse model [98] for polymers in eq. 13 where γ is a force constant uniform for all springs, and Γ_{ij} is the ij-th element of the Kirchhoff matrix of inter-residue contacts (eq. 14-15).

$$V_{GNM} = \frac{\gamma}{2}\left[\sum_{i,j}^{N}(\Delta R_j - \Delta R_i)^2\right] = \frac{\gamma}{2}\left[\sum_{i,j}^{N}\Delta R_i \Gamma_{ij}\Delta R_j\right] = \frac{\gamma}{2}\Delta R \Gamma \Delta R \tag{13}$$

Force constant   **Fluctuation vector ΔR**   **Kirchhoff matrix Γ_{ij}**

$$\frac{\gamma}{2}[\Delta R_1 \quad \Delta R_2 \quad \Delta R_3 \quad ... \quad \Delta R_{N-1} \quad \Delta R_N]\begin{bmatrix} 1 & -1 & & & & \\ -1 & 2 & -1 & & & \\ & -1 & 2 & & & \\ & & & ... & & \\ & & & -1 & 2 & -1 \\ & & & & -1 & 1 \end{bmatrix}\begin{bmatrix} \Delta R_1 \\ \Delta R_2 \\ \Delta R_3 \\ ... \\ \Delta R_{N-1} \\ \Delta R_N \end{bmatrix} \tag{14}$$

$$\Gamma_{ij} = \begin{cases} -1, & if\ i \neq j\ and\ R_{ij} \leq r_c \\ 0, & if\ i \neq j\ and\ R_{ij} > r_c \\ -\sum_{j,j\neq i}^{N}\Gamma_{ij}, & if\ i = j \end{cases} \tag{15}$$

In contrast to GNM, which is limited to the evaluation of the mean squared displacements and cross-correlations between fluctuations where the motion is projected to a mode space of N dimensions, the ANM concept permits us to evaluate directional preferences by providing 3D descriptions of the *3N-6* internal modes. Therefore in ANM, the force constant of the system is described by the Hessian matrix *H,* which is composed of the second partial derivatives of the potential *V* (eq. 16).

$$H = \begin{bmatrix} H_{11} & H_{11} & .. & H_{1N} \\ H_{21} & H_{11} & .. & H_{1N} \\ & .. & .. & \\ H_{N1} & .. & .. & H_{NN} \end{bmatrix} \tag{16}$$

$$H_{ij} = \begin{bmatrix} \dfrac{\partial^2 V}{\partial X_i \partial X_j} & \dfrac{\partial^2 V}{\partial X_i \partial Y_j} & \dfrac{\partial^2 V}{\partial X_i \partial Z_j} \\ \dfrac{\partial^2 V}{\partial Y_i \partial X_j} & \dfrac{\partial^2 V}{\partial Y_i \partial Y_j} & \dfrac{\partial^2 V}{\partial Y_i \partial Z_j} \\ \dfrac{\partial^2 V}{\partial Z_i \partial X_j} & \dfrac{\partial^2 V}{\partial Z_i \partial Y_j} & \dfrac{\partial^2 V}{\partial Z_i \partial Z_j} \end{bmatrix}$$

More details of GNM and ANM concepts can be found in extensive reviews [95, 99-105].

Based on the ENMs concept, we can obtain different types of analysis which were successfully used to obtain results present in the achievement, e.g.:

- *Cross-correlation* between residue motions (eq. 17) is defined by the Kirchhoff matrix (connectivity matrix, Γ_{ij}, N×N in the GNM) to analyze protein structures to infer their dynamical properties and predict regions that will exhibit highly correlated (values ~0.7 to 1) and anti-correlated (-0.75 to -1) motions. Non-correlated regions (values ~0) are called hinge sites and play a significant role in predicting potential inhibitory binding sites that may affect collective protein motions, thus leading to the loss of protein function. This approach helps to identify potential allosteric sites in the protein structures [**H1**, **H3-H4**][**A3**].

$$< (\Delta R_i \cdot \Delta R_j) > \sim [\boldsymbol{\Gamma^{-1}}]_{ij} \qquad (17)$$

- *Perturbation Response Scanning (PRS)*, adopted to GNM (eq. 18-19), is based on the linear response theory [106] and allows to evaluate of residue displacements in response to external forces **F** to predict the effectiveness and sensitivity of residues for allosteric signal transduction within the protein structure [107-109][**H4**][**A3**]. The strongest effectors can be interpreted as elements that apply global control over the propagation of allosteric signals to a partner (protein/ligand). The strongest sensors define effective receivers of allosteric signals involved in the execution of allosteric structural changes. In this concept, the *i*-th element of $\boldsymbol{\Delta R_i}$ designates displacement of the *i*-th residue away from its equilibrium position in response to the exerted force **F**. Next, we evaluate the response $\boldsymbol{\Delta R_i}$ of all residues to a unit force applied to the *j*-th site using the operation, $\boldsymbol{\Gamma^{-1} F_j}$, where $\boldsymbol{F_j}$ is composed of all zeros except for the *j*-th element that is equal to one. Repeating (scanning) this procedure for all sites yields a response matrix [**H4**].

Perturbation   **Response**

$$\gamma^{-1} \boldsymbol{\Gamma^{-1}} \boldsymbol{F} = \Delta \boldsymbol{R} \qquad (18)$$

$$\gamma^{-1} \boldsymbol{\Gamma^{-1}} \begin{bmatrix} \boldsymbol{F}_1 \\ \boldsymbol{F}_2 \\ \boldsymbol{F}_3 \\ ... \\ \boldsymbol{F}_{N-1} \\ \boldsymbol{F}_N \end{bmatrix} = \begin{bmatrix} \Delta \boldsymbol{R}_1 \\ \Delta \boldsymbol{R}_2 \\ \Delta \boldsymbol{R}_3 \\ ... \\ \Delta \boldsymbol{R}_{N-1} \\ \Delta \boldsymbol{R}_N \end{bmatrix} \qquad (19)$$

- *Signature dynamics (SignDy)* to evaluate characteristic features of a protein family dynamics and to classify proteins based on their collective dynamics [110][**H4**].

- *Mechanical Stiffness calculations (MechStiff)* to determine mechanical resistance to external force, i.e., uniaxial tension applied at specific pairs of residues in the protein structure. This concept uses ANM to construct a map of the mechanical response of all residue pairs in a given protein to uniaxial deformation. The theory is introduced and described in detail in [105], and application to protein structure can be found in [**H4, A4**].

ProDy. The analysis applied to obtain the results for the achievement was written in *Python* code in the *ProDy* package [111, 112][**A6**]. As a postdoc in Prof. Ivet Bahar lab, I participated in developing this open-source package [**A4-A6**] that is extensively used by the scientific community (>2.3 mln downloads). I provided >2 200 lines of code, which were included in *ProDy* (*Github* data), and >50 000 lines of code which were used in independent scripts shared with other scientists via *Supplementary Materials* in published publications.

IV.3.3. Results and description of publications

The habilitation achievement concern enzymatic aspects of the RCD program called ferroptosis, and it is focused mainly on the lipoxygenases (LOXs) that are giving the biggest contribution to the generation of lipid peroxides causing massive lipid peroxidation and membrane damage in that process. The achievement includes two main directions/goals:

    A.   to decipher the molecular basics of ferroptosis related to lipid peroxidation generated by lipoxygenases 15LOXs, and

    B.   to inhibit the ferroptosis process by acting on 15LOXs structure or its products.

For this reason, I will discuss the papers in thematic groups concerning molecular mechanisms of ferroptosis at the atomic level and inhibition studies using (i) nitric oxide, (ii) ferrostatin-1, which is the most common ferroptosis inhibitor, and eventually, (iii) phospholipase role in the hydrolysis of lipid hydroperoxides that are generated by 15LOX complex with PEBP1.

A. Exploring the fundamental mechanisms of the ferroptosis process

Human lipoxygenases. A number of LOX-knock out cells experimental studies showed controversial results, which only partially confirm the involvement of lipoxygenases [113, 114] in the ferroptosis process, suggesting that yet another factor is needed for the PUFA-PL peroxidation. Indeed, in [**H1**] we discovered that ferroptosis is a cell death program executed via selective oxidation of SA-PE by 15-lipoxygenase (both isoforms: 15LOX-1 and 15LOX-2) complexed with a protein called PEBP1, and this complex promote ferroptosis [**H1**].

PEBP1 is a highly important regulatory protein that is involved in different kinds of RCD programs [115]. It has been shown in numerous studies that PEBP1 interacts not only with lipids [116, 117] or small molecules [118] but also with a diverse number of RCDs-associated proteins, such as RIP3 (necroptosis [115]), Raf-1 (necroptosis [115]), and LC3 (autophagy [119][**A1**]). We showed the importance of PEBP1 in the regulatory mechanism of yet another RCD program – ferroptosis – in airway epithelial cells in asthma, kidney epithelial cells in renal failure, and brain trauma [**H1**]. We revealed that upon PEBP1 binding, human 15LOX changes its substrate specificity from classical LOXs substrate, i.e., free PUFA [51] (AA) to esterified PUFA-PL (SA-PE) to generate hydroperoxy-PE (also called 15-HpETE-PE) which is used as a cell death signal of ferroptosis [**H1**].

In order to provide insight into the molecular level of different components of the ferroptosis machinery, I employed computational biophysics tools to generate structural models of the human 15LOX/PEBP1 complex using molecular docking simulations [**H1**]. Prediction of the physical models of the human 15LOX/PEBP1 complex provided detailed information about their binding interfaces and their physical interactions within residue pairs (**Fig. 9A** (15LOX-1 (*upper panel*) and 15LOX-2 (*bottom panel*)) [**H1**]. That information was further used to suggest potential mutations (e.g., P112E in PEBP1) and modifications (a truncation of the C-term helix, **Fig. 9,** *bottom panel*) in PEBP1 structure to verify the proposed computational model in mutagenesis studies performed by the collaborators [**H1**].
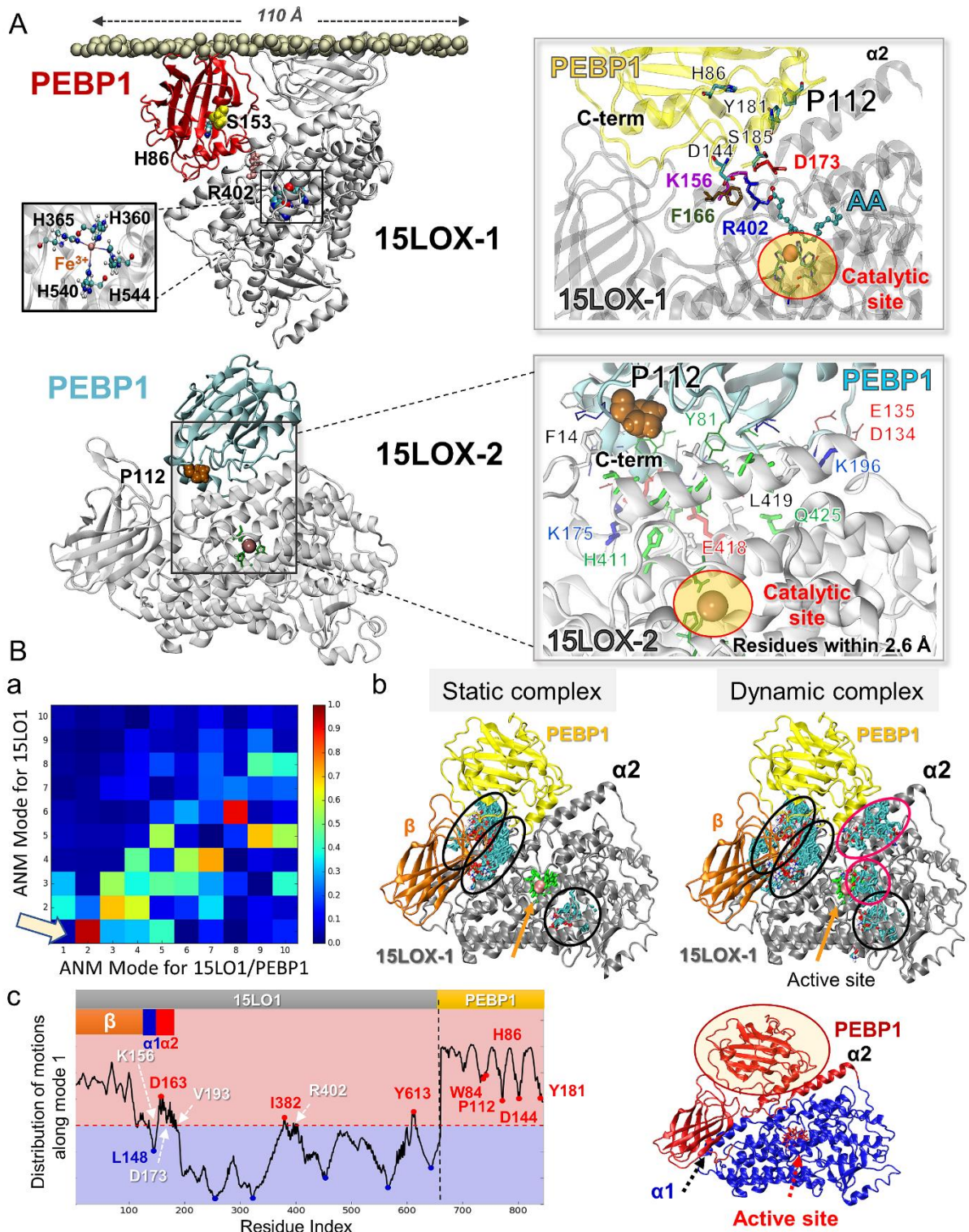
Figure 9. Structural model and collective dynamics of the human 15LOX complexed with PEBP1. *(A) 15LOXs (15LOX-1 and 15LOX-2) structural models in a complex with PEBP1. The insets provide close views of the binding interfaces. (B) Elastic Network Model analysis: (a) Correlation cosines between the ANM modes of motions accessible to 15LOX-1 in unbounded (ordinate) and bounded form with PEBP1 (abscissa). The correlations are color-coded from red (strongest) to blue (weakest). (b) Comparison of binding poses of SA-PE onto the PEBP1/15LOX-1 complex, obtained for the rigid/static complex (left panel) and dynamic/flexible complex along ANM mode 1 (right panel). Two additional hotspots (pink ovals) were observed when the complex is allowed to reconfigure along mode 1. (c) GNM mode profile which shows the relative motions of different 15LOX-1 regions in a complex with PEBP1. Positive (red) and negative (blue) regions indicate the structural regions subject to anti-correlated (coupled but opposite*

16

direction) motions. The spatial model of the complex is color-coded by substructures that undergo anticorrelated movements in the GNM principal mode. Source: mainly [**H1**] *collected from different figures.*

Proteins are dynamic objects that undergo structural transitions. These are essential to their functions but not fully captured by the experimental studies (crystallography, NMR), which provide only a small number of structural poses that are deposited in the PDB database. To obtain information about the long-term collective dynamics of the 15LOX-1/PEBP1 complex, I used elastic network models (GNM and ANM) to provide a possible explanation of why the substrate specificity of 15LOX-1 can change upon binding with PEBP1. My ANM predictions imply that after complexation with PEBP1, 15LOX-1 gains a new low-frequency mode which may change LOX specificity, and this mode is not accessible for 15LOX-1 alone (**Fig. 9Ba**, Video in [**H1**]). Molecular docking applied to the 15LOX-1/PEBP1 conformations, which were changing along the predicted ANM mode, showed differences in SA-PE binding and accessibility to new binding spots localized closer to the catalytic site (*pink ovals*, **Fig. 9Bb**). Moreover, the complex formation affects the relative motions of different regions of 15LOX-1 along the principal mode of GNM motion compared to the isolated 15LOX-1 (**Fig. 9Bc**).

Afterward, we studied the effects of PEBP1 on the enzymatic oxidation of free AA. In the absence of PEBP1, 15LOXs exert high activity toward free AA than for SA-PE [**H1**]. Everything is changing in the presence of PEBP1. Therefore, we tested PEBP1 capacities of AA binding using its two models, native structure (WT) and its mutant (Y176X with truncated C-term helix starting from Y176), including experimental and computational approaches. The experimental studies detected three, six and nine binding spots for WT PEBP1. Therefore, I predicted up to nine possible binding sites, which were further verified by all-atom MD simulations (7 poses stayed stably retained) [**H1**]. Experiments demonstrated that deletion of the C-terminal helix of PEBP1 greatly reduced AA binding, and that was also implied by the computational studies for Y176X PEBP1 (figures[1]: *Fig.6F, Fig. S6A,C;* available in [**H1**]). In this studies, my work was guiding and supporting experimental studies by providing molecular explanation of the mechanisms that may occur in the biochemical systems.

Our next [**H2**] paper provided a possible explanation for why the enzymatic complex of 15LOX-2 and PEBP1 selects SA-PE substrate among ~100 total oxidizable membrane phospholipids. To uncover the selective and specific mechanisms of catalytic competence, we used redox lipidomics, mutational analysis, and computational biophysics to reveal that they are related to (i) reactivity toward readily accessible membrane with SA-PEs, (ii) the relative preponderance of PUFA PE species compared to the other PUFAs, and (iii) allosteric modification of human 15LOX-2 upon complexation with PEBP1.

Computational modeling was involved in explaining the allosteric modulation of 15LOX-2 after PEBP1 binding [**H2**]. I combined two approaches, molecular docking, which provides the binding affinity of two structures (in this case, 15LOX-2/PEBP1 complex and SA-PE), and normal mode analysis, which predicts collective modes of protein assemblies (15LOX-2/PEBP1 complex). The goal was to show how the substrate binds to the catalytic site of 15LOX-2 in bound form with PEBP1 upon movement of ANM global mode 1 (Video in [**H2**]). This approach was used to show that low-frequency mode appeared upon PEBP1 interactions with 15LOX-2. We

---

[1] Figure references in italics refer to figure numbers in [**H1-H8**] publications.

observed movements of the flexible helix decreasing the active site entrance hence restricting accessibility for lipids with large head groups (PI and PC) but not for PE lipids [**H2**].

Bacterial lipoxygenase. We showed that ferroptosis is a regulated cell death program that can be executed via selective SA-PE oxidation by human 15LOX/PEBP1 complex [**H1-H2**]. 15LOXs are widely represented in many eukaryotic cells [120, 121], however, they are also present in prokaryotic bacteria [122, 123]. Therefore, we conceived studies that included 15LOX from the bacteria *Pseudomonas aeruginosa,* which is considered as a pathogen with high medical importance. Firstly, because it is commonly found in natural environments such as soils, plants or waters and causes diseases not only in humans but also in plants and animals [124]. Secondly, because the World Health Organization (WHO) included *P. aeruginosa* in the WHO list of the critical priorities due to its infecting abilities and multidrug resistance [125].

We showed in [**H3**] that *P. aeruginosa* had developed a capacity to use a unique enzyme, 15-lipoxygenase (called pLoxA or PA-LOX), to hijack the ferroptotic death program, i.e., utilize host polyunsaturated SA-PE to trigger theft-ferroptosis in the bronchial epithelium cells which not only destroy the epithelial barrier but may compromise immune-stimulating functions [**H3**]. Surprisingly, this type of bacteria does not contain PEBP1 or SA-PE lipids in its system, but still, it is able to express pLoxA, oxidize host SA-PE to 15-HpETE-PE, and trigger ferroptosis in humans. Experiments on samples isolated from patients with persistent lower respiratory tract infections, provided by collaborators, showed high levels of oxidized SA-PE in patients with cystic fibrosis [**H3**], in which *P. aeruginosa* causes long-term chronic airway infections, often lasting for years. This evolutionarily conserved mechanism, detected in [**H3**] studies, i.e., pLoxA-driven ferroptosis, might be a potential therapeutic target to treat patients with pathology of cystic fibrosis which represents the most common autosomal recessive disease (Caucasian population; 1/3500 births) [126].

To provide a detailed explanation at the molecular level, I used computational biophysics approaches and structural models of bacterial pLoxA and human 15LOX/PEBP1 complexes to explain why pLoxA can trigger ferroptosis without PEBP1 [**H3**]. Based on the detailed analysis of the structural alignment of eukaryotic and prokaryotic 15LOX structures, I have identified special features of the human 15LOXs members that are also conserved in pLoxA structure and required for the oxidation process of SA-PE, however, not noticeable via sequence alignment (**Fig. 10A**, *highly conserved residues in blue* and *Fig. S7A* in [**H3**]). I also showed that despite the large structural similarity of the prokaryotic and eukaryotic models, pLoxA has two additional helices which are absent in the mammalian 15LOXs (**Fig. 10B**). Normal mode analysis using GNM implied that those additional helices may serve in pLoxA as a lid and additionally modify the organization of the catalytic site to favor the binding of bulkier substrates, such as SA-PE instead of AA, just like PEBP1 for the human 15LOXs (**Fig. 10C**). Moreover, I showed that the softest ANM mode (global mode 1) disclose the passage between substrate-bound and unbound structure provided by the crystallography and deposited in PDB (Video in [**H3**]). It additionally demonstrates the reliability of the predicted movements/modes by the elastic network models.
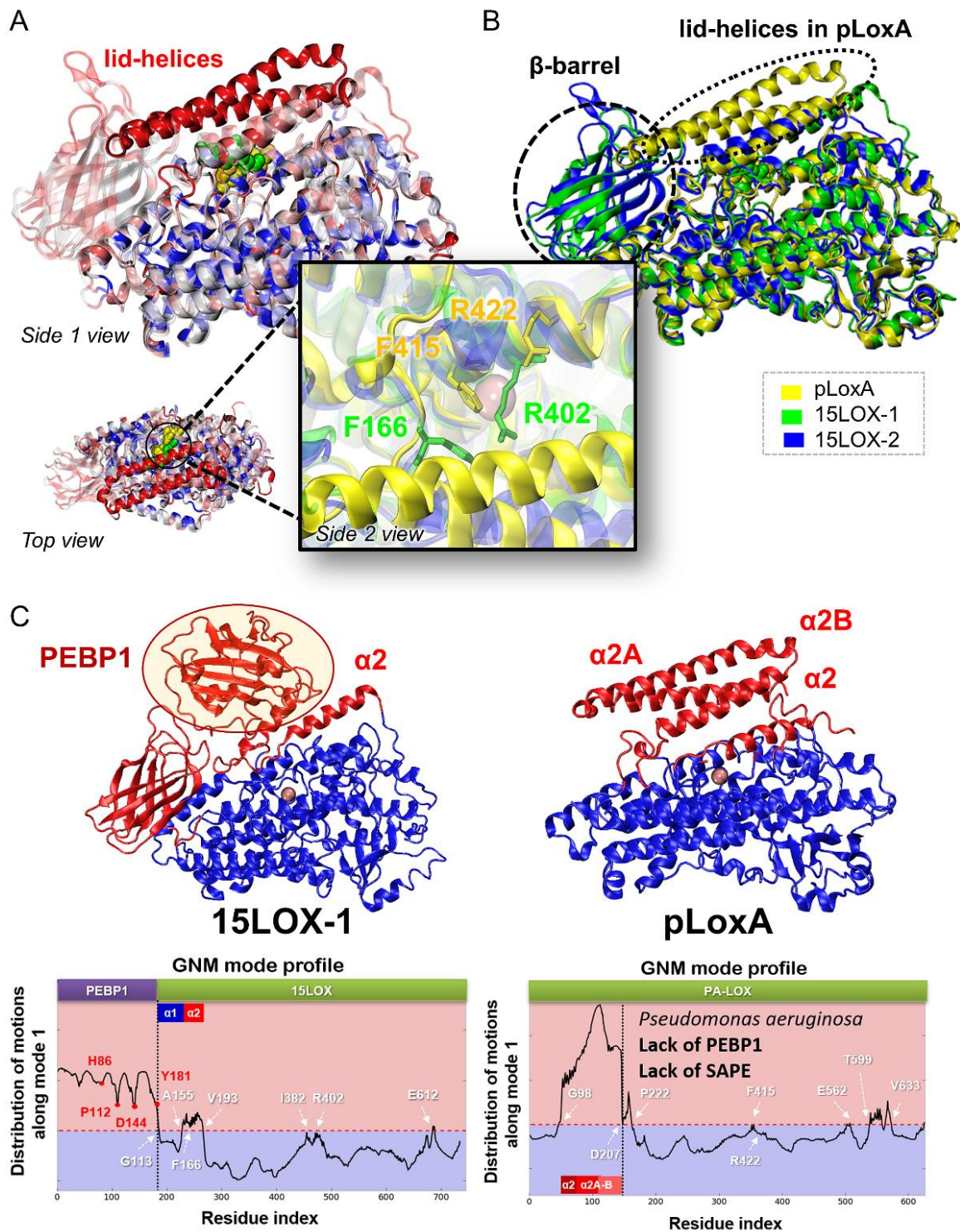
Figure 10. Dynamics and sequence conservation of pLoxA structure and its comparison with the human form. *(A) Ligand-binding site in pLoxA structure, and comparison of a pair of Arg-Phe, represented by both bacterial and mammalian LOXs. The structure is colored by the sequence conservation (red-white-blue) based on the LOXs family members. (B) Structural comparison of pLoxA and mammalian LOXs (15LOX-1 and 15LOX-2). The structural alignment displays the missing β-barrel of the bacterial pLoxA and its two additional α-helices, (C) Comparison of the GNM global motions of pLoxA and 15LOX-1 complexed with PEBP1. Displacements of residues along the global mode axis obtained from GNM analysis of 15LOX-1/PEBP1 complex (left panel) and pLoxA (right panel) dividing the structure into two domains that exhibit anti-correlated motion. Residues at the hinge sites (crossover region, in white) are labeled. The correlated groups of residues are shown in red or blue. Source:* [**H3**].

Next, I used all available LOXs sequences from the Pfam [127] database (>230 sequences of LOXs; raw data prepared by Dr. James Krieger in the evolutionary analysis of LOXs sequences) to display the pairwise sequence identities and a corresponding phylogenetic tree with the particular emphasis on different bacteria (*Fig. S8* in [**H3**]). It revealed the tendency of residues located near the catalytic site of LOXs to be conserved, whereas peripheral regions, including additional helices that distinguish pLoxA from mammalian 15LOXs, exhibited significant sequence dissimilarity.

We looked more closely at the whole LOXs family, particularly the structural properties and dynamics, which may give detailed information about signal transduction, correlation, and functionality of different protein regions [**H4**]. Such modeling across different species and types can help to understand the mechanisms of actions shared by family members as well as the specificity assigned to individual members, e.g., why 15LOX-2 demonstrates specificity toward inserting O_2 exclusively at C15 position of PUFA and 12LOX at C12 and occasionally at C15, or why some LOXs prefer linoleic acid (LA) and not above mentioned as a preferable substrate, arachidonic acid (AA).

In this fully computational study, we used structure-based models and methods together with bioinformatics tools to analyze 88 available crystal structures of LOXs deposited in the PDB database, and we classified LOX family members based on their: (i) sequence, (ii) structure, (iii) dynamics, and (iv) allostery. I performed all the computations and most of the analysis in [**H4**] study, and due to their extensiveness, only the main points will be presented here.

In [**H4**], I estimated that among LOX family members, the sequence identifies (SID) is relatively small (SID: 28.6 ± 3.7 Å, **Fig. 11A**), but at the same time, the family shares a similar fold (RMSD ~2.3 Å, **Fig. 11B**). The largest structural variation occurs at the β-barrel domain and the lid helices [**H3-H4**]. Next, based on the newly developed by Dr. J. Krieger, Dr. S. Zhang, and Dr. H. Li (co-authors of [**H4**]) ProDy module (*SignDy*), I computed signature dynamics plot, e.g., mean-square fluctuations of residues for the whole LOX family based on available crystal structures (**Fig. 11C**, *blue curve*) and its standard deviation (*light blue band*). This type of analysis provides similarities (low standard deviation, **Fig. 11C**) and differences (high standard deviation, **Fig. 11C**) among a particular family of proteins based on their dynamics estimated from ENMs, in our case, ten low-frequency modes of GNM. The analysis revealed that the functional sites (catalytic residues, highly important sequence motifs, e.g., WxxAK, WxxD) undergo minimal movement (occupy minimum in **Fig. 11C**, *yellow boxes*) due to the tight orientation that is required for the enzyme's mechanochemical activity [128]. Also, the collective dynamics is shared among all LOXs (narrow band in **Fig. 11C**) except five peak regions denoted by colored bars along the upper abscissa and displayed on the spatial structure of pLoxA (**Fig. 11C**, *in red* on the *right panel*). Detailed analysis of low- (*left panels*) and high-frequency (*right panels*) modes showed differences between different LOX species (**Fig. 11D**). Notably, *Region 5* may help to customize the precise positions of specific substrates at the catalytic site (as implied in [**H2**]). Its anticorrelated motion may be facilitating access of putative oxygen assess the catalytic site (shown in [**H5-H6**] to be *Entrance 1* for 15LOX-2) with the conserved blocks including the WxxAK and WxxD motifs (*Fig. S3* in [**H4**]). Further, based on the similarities of the collective dynamics of individual LOX, I was able to provide subgroups within LOX family members, e.g., group them based on the dynamics (**Fig. 11E**).
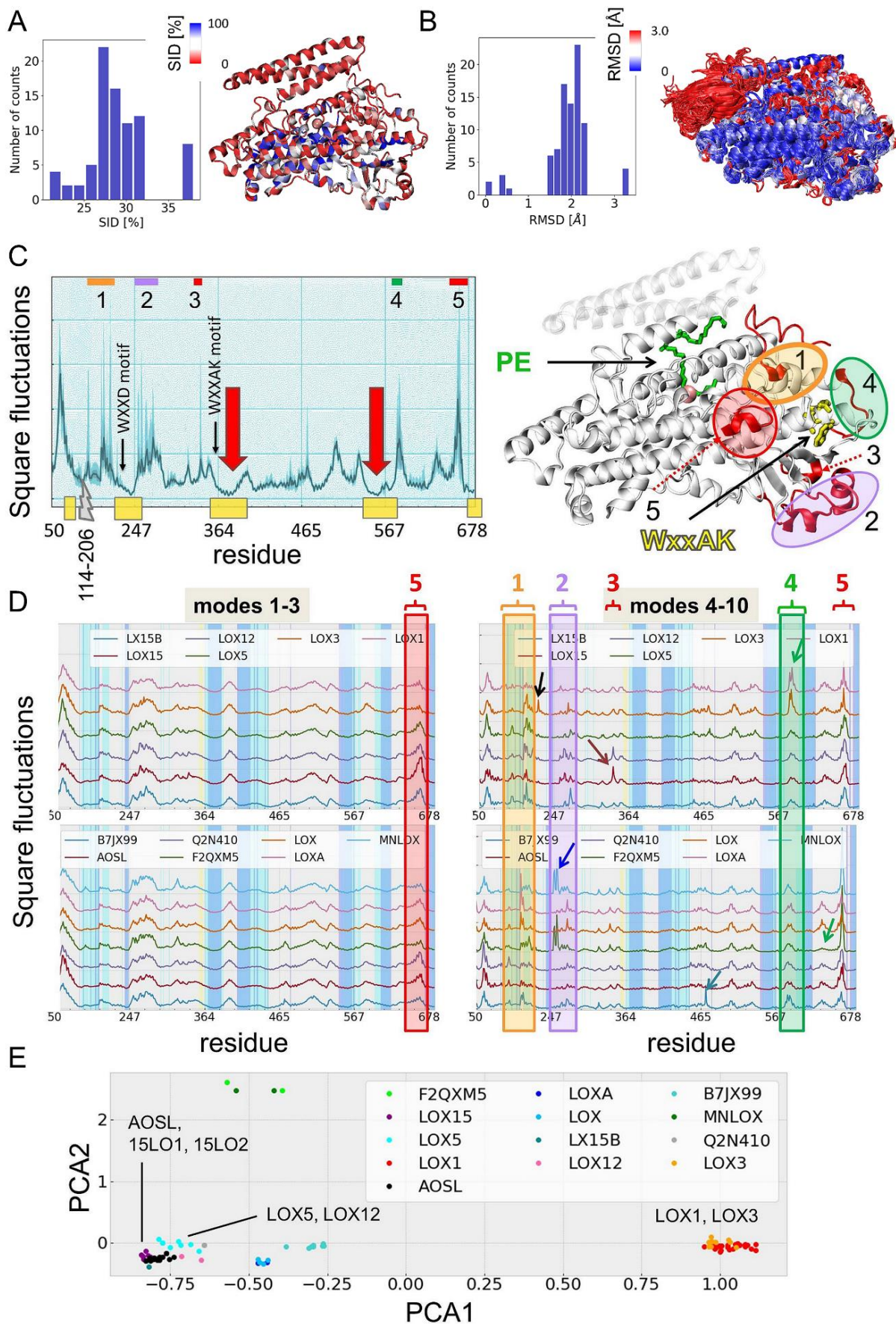
Figure 11. Sequence and structure properties of the LOX family members deposited in the PDB database. (A) Histogram of sequence identity (SID) and corresponding SID per residue displayed on

the spatial structure of pLoxA. (B) Distribution of RMSDs and structural alignment of LOX structures, (C) Signature dynamics plot for LOX family members. Results are based on 88 PDB structures. Regions 1−5 (high peak regions) shown on the representative pLoxA structure are centered around D207-R211, I250-E276, A338, S585-S588, and A666-R668. WxxAK motif comprising residues W357-K361 in pLoxA. (D) Low-frequency modes (modes 1-3) and high-to-intermediate frequency modes (modes 4-10) for 13 representative LOX family members. (E) Distribution of LOXs in the subspace spanned by the two principal components obtained by PCA. Source: [**H4**].

The data presented above was a basis for conducting other essential ENM-based analyses that provided similarities and variations among LOX family members. All the analyses, including cross-correlation between the spatial fluctuations of different regions in LOX members (*Fig. 3 and Fig. S3* in [**H4**]) and the PRS which evaluate the role of LOX residues as sensors and effectors of allosteric signals in the LOX family (*Fig. 4* in [**H4**]) imply the significance of *Region 5*. The unique role of *Region 5* was also noticed in the Mechanical Stiffness analysis based on ANM (implemented as the *MechStiff* module by myself in ProDy), which calculates the resistance of all residue pairs to uniaxial tension (*Fig. S5* in [**H4**]). Notably, especially clear we could see it in MD simulations (*Fig. S4* in [**H4**]) of the human 15LOX-1/PEBP1 complex where before PEBP1 binding, 15LOX-1 residues at the PEBP1-interface exhibits high sensitivity features (potential binding place for a partner in PRS), and after complexation with PEBP1 this feature is transmitted to *Region 5*. In [**H4**], I performed the first all-atom MD simulations of the human 15LOX-1/PEBP1 complex with a fully parametrized catalytic site of 15LOX-1 (using quantum calculations) [**H4**]. After checking the dynamic (**Fig. 11**) and structural (*Fig. S1* in [**H4**]) variability of the LOX family, we focused on the sequence conservations among LOXs in different species (human – *Fig. S2* in [**H4**]), including their characteristic and dynamically highly stable motifs (*Fig. 5* and *Fig. S1* in [**H4**]).

B. Inhibition of a ferroptotic cell death signal

Understanding how cells die in the ferroptosis process presents an enormous translational potential by offering opportunities to control a ferroptotic-associated cell death or survival. Ferroptosis has been associated with the pathogenesis of many severe diseases. This explains the high interest in designing new inhibitors and prevention methods against ferroptosis. The goal of present scientific achievement was not only to decipher the mechanisms that control the enzymatic aspect of ferroptosis but also to find a sufficient way to inhibit it, especially by interfering in the lipid peroxidation process associated with 15LOX/PEBP1 complex [**H1-H3**]. We considered four approaches, described below, that may significantly affect the production of lipid hydroperoxides that lead to ferroptosis, i.e.

(i)   using nitric oxide (NO) to affect the production of lipid hydroperoxides by human 15LOX/PEBP1 complex [**H5-H6**],

(ii)   affecting the human 15LOX/PEBP1 complex formation upon ferrostatin-1 (Fer-1) binding [**H7**],

(iii)   eliminating lipid hydroperoxides which are produced by the 15LOX/PEBP1 complex in the hydrolysis process before peroxidation cascades will appear [**H8**],

(iv)   finding new inhibitors of 15LOX/PEBP1 complex (manuscript submitted to PNAS).

Nitric Oxide (i) The production of lipid hydroperoxides by LOXs, as indicated in **Fig. 4**, take place in the presence of iron and needs an O_2 molecule to be inserted in the PUFA tail, which is rich in bisallylic methylene carbon. We showed in our previous studies [**H1-H3**] that the 15LOX/PEBP1 complex, rather than 15LOX alone, catalyzes the oxidation of SA-PE, therefore, we focused in turn mainly on the 15LOX-2/PEBP1 complex [**H5**] and its bound form with the preferable substrate, SA-PE [**H6**]. In order to check whether nitric oxide (NO) molecules may act as effective regulators of ferroptosis, we conceived studies that include NO interactions with the above-mentioned complex. Experimentally, we showed that an enzyme inducible nitric oxide synthase (iNOS), which catalyzes the production of NO [129], demonstrates potency to directly control ferroptosis in macrophages and microglia through NO act in suppressing the production of 15-HpETE-PE by 15LOX-2/PEBP1 complex, and all explanation on the molecular level was provided by my computational work [**H5-H6**].

Using all-atom MD simulations, I showed how NO competes with O_2 [Videos in [**H5**] (substrate unbound) and [**H6**] (substrate bound), *Fig. 3* in [**H6**]] for a binding site of 15LOX-2, providing all the details of crucial interactions at the molecular level. It results in suppressing the production of 15-HpETE-PE by the human 15LOX-2/PEBP1 complex while promoting the formation of nitrosylated ETE-PE, i.e., NO instead of O_2 is inserted in the PUFA tail [**H6**].

MD findings presented in [**H5-H6**] provide the description of NO inhibition and extend our understanding of the ferroptosis mechanism by identifying the specific interactions and mechanisms of LOXs activation. I characterized here O_2 and NO diffusion pathways, that take a place in the catalytic cycle of human 15LOX-2 to generate lipid hydroperoxides (**Fig. 4**). I performed MD simulations of 15LOX-2 in bound/unbound form with PEBP1 and SA-PE (SA-PE unbound form [**H5**] and SA-PE bound form [**H6**]) which revealed functional channels (referred as "*Entrance*" in **Fig. 12-13**) that are guiding O_2 and NO to the catalytic site of 15LOX-2 (**Fig. 12A-B**, **Fig. 13B-C**) and those which participate in the NO/O_2 interactions when the oxidation process appears (**Fig. 13D**). Next, I showed that *Entrance 1* is the main oxygen channel (near residues Y154, N155, W158) to the catalytic site and *Entrance 2* is almost completely covered in the presence of PEBP1 (**Fig. 12B**). In substrate bound simulations, I observed additional channel, *Entrance 3*, which was not observed in the simulations without the substrate (**Fig. 13B**).

Moreover, I identified the specific interactions (*Fig. 5-6* and *Fig. S4* and *Table S2* in [**H6**]) and mechanism of activation of 15LOX upon binding with PEBP1, which could not be fully understood without computational structure-based studies (**Fig. 14**). My studies also revealed an additional role of PEBP1 which upon interaction with 15LOX-2 change a conformation of a loop localized at the PEBP1/15LOX-2 binding site (**Fig. 14A**, *in orange*), thus resulting in increasing the affinity of NO to the catalytic site. In the absence of PEBP1, at low NO concentrations, NO molecules were unable to access the catalytic site being attracted by the cavity near the sn-2 chain of SA-PE (**Fig. 14B-C**, *Fig. S6-S7* in [**H6**]). That knowledge was critical to explain experimental findings on how and why NO molecules inhibit ferroptosis at high concentrations in the presence of PEBP1. Thus, a critical role of PEBP1 in the ferroptosis process was confirmed [**H6**].
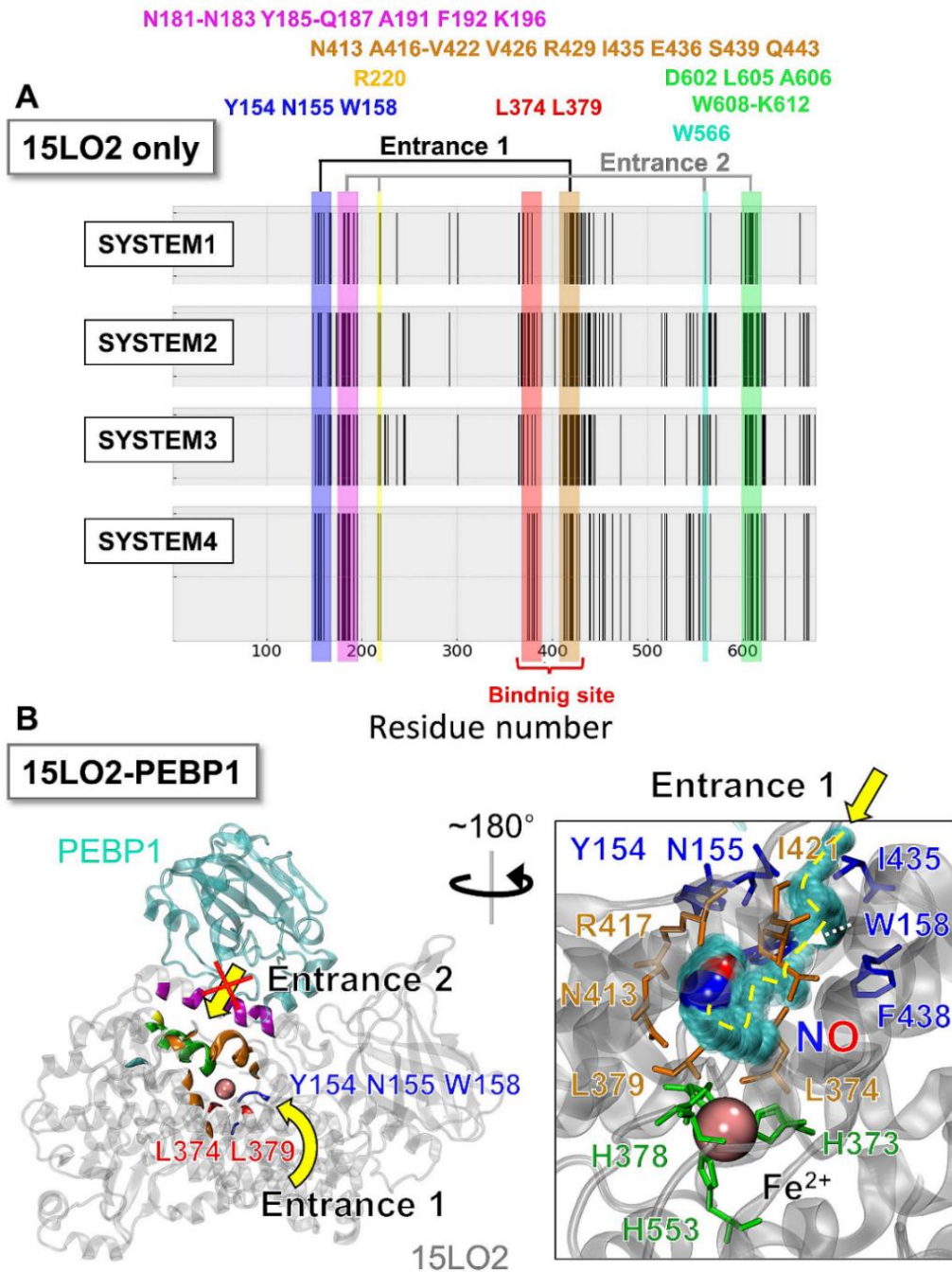
Figure 12. All-atom MD simulations of the human 15LOX-2/PEBP1 complex. *(A) NO and O_2 close contracts during MD simulations (4 trajectories), (B) Crystal structure of 15LOX-2/PEBP1 complex with regions of the most frequent NO/O_2 interactions, color-coded in the same scheme as in panel (A). In the inset, the close view of the diffusion pathway for NO/O_2 molecules through Entrance 1. Entrance 1 residues (in blue), crucial interactions at the catalytic site (in orange), and catalytic residues (in green) are displayed. Source:* [**H5**].
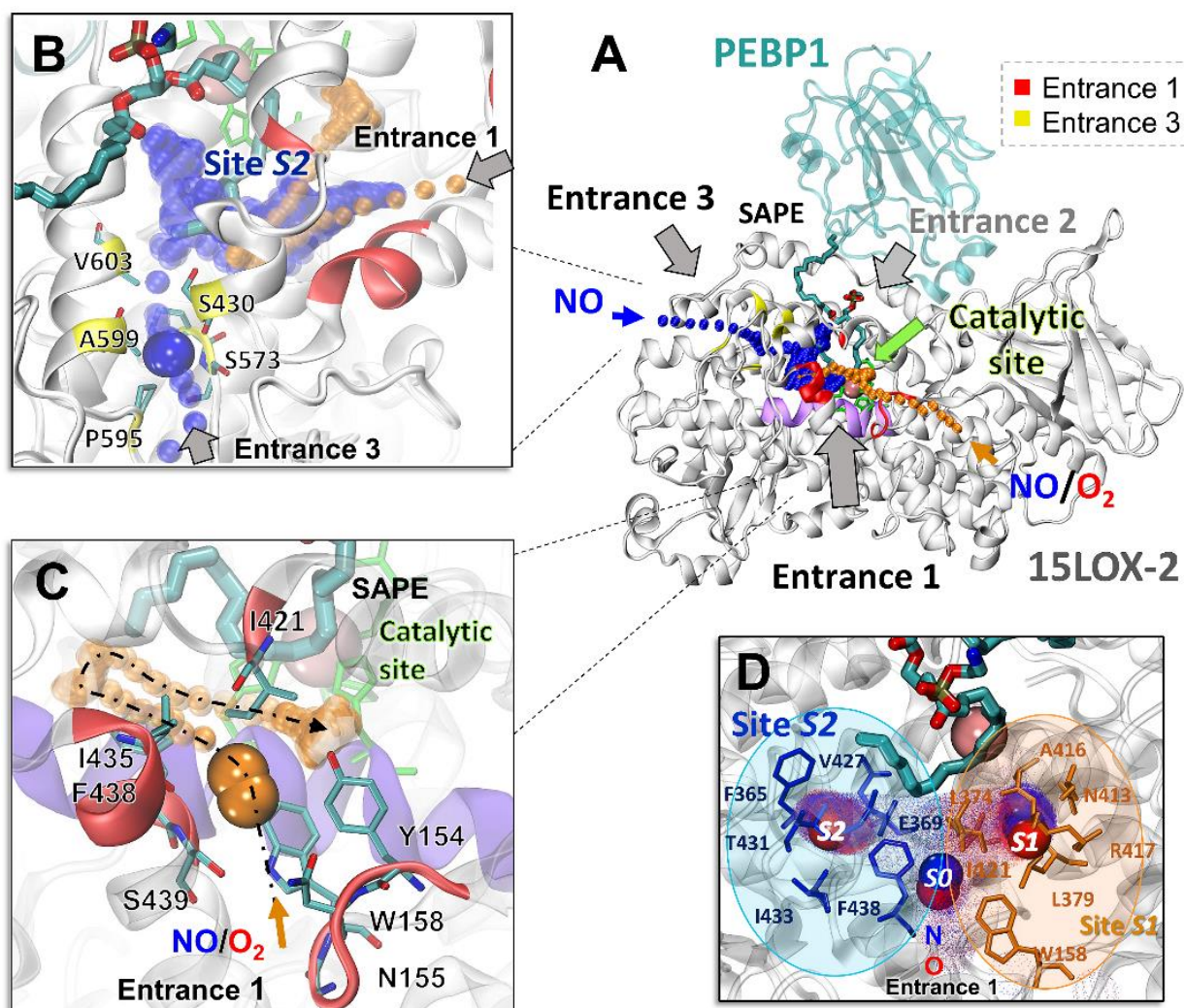
Figure 13. All-atom MD simulations for the human 15LOX-2/PEBP1/SA-PE complex revealed functional O₂/NO channels to the catalytic site of LOX. *(A). Crucial residues for Entrance 3 (B) and Entrance 1 (C, S0 site in D) are displayed. Entrance 2 (A) is closed due to PEBP1 and substrate SA-PE. NO/O₂ molecules occupy two binding sites at the catalytic site close to the substrate (S1 and S2). Source:* [**H6**].
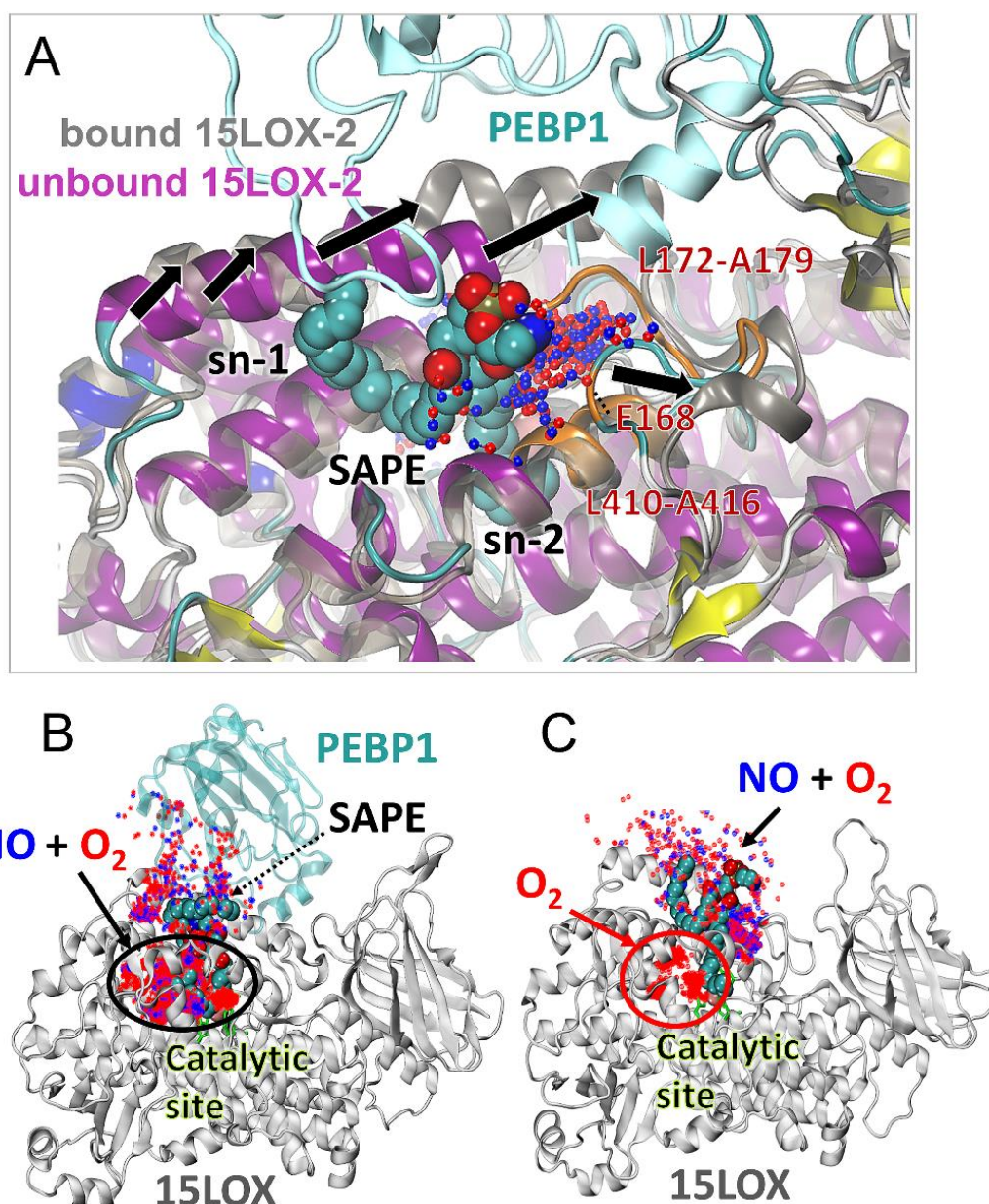
Figure 14. MD simulations for 15LOX-2/PEBP1 complex (A) and 15LOX-2 (B) predicted a conformational change in LOX induced upon PEBP1 binding, which allows nitric oxide (NO) binding to the catalytic site in the presence of SA-PE (C). Source: [**H6**].

Ferrostatin-1 (ii) Ferrostatin-1 (Fer-1) is the most commonly used ferroptosis inhibitor, applied to ~15-20% of all experiments reported in publications. Some studies indicate that this anti-ferroptotic agent is a poor 15LOX inhibitor [113, 130]. That claims were causing scientific disputes among researchers supporting the concept of enzymatically driven ferroptosis. It has been implied that probably free radical lipid peroxidation (i.e., Fenton reaction, **Fig. 2-3**) rather than enzymatic LOX-driven reaction (**Fig. 2**, **Fig. 4**) is essential for executing the ferroptotic cell death process.

Our [**H7**] study explained this unsolved paradox of the ferroptotic cell death, which indicate that the anti-ferroptotic agent, Fer-1, is a poor 15LOX inhibitor, i.e., to an enzyme that is giving the biggest contribution to the generation of lipid hydroperoxides. To elucidate this unsolved

scientific riddle, I first used molecular docking to determine Fer-1 binding sites in the 15LOX-2 structure in the bound/unbound form with PEBP1. This approach gave not only the binding affinity of individual ligands (enthalpy) but also revealed more entropically favorable sites of the complex by exposing high populations of Fer-1 bonded poses (**Fig. 15A** – unbound 15LOX-2, **Fig. 16A** – bound 15LOX-2). Additionally, this approach included multiple conformations of the protein ensemble extracted from previously performed all-atom MD simulations using PCA and the Mean Shift algorithm [**H7**]. This extensive docking on multiple protein(s) conformations (in total >900 Fer-1 binding poses) was used to distinguish differences in Fer-1 binding in the presence of PEBP1 (**Fig. 15B**, **Fig. 16B**).

Three conformations of Fer-1 with the lowest energy of binding (the highest binding affinity, **Fig. 16B**, *Site 2* and *Fig. S4* in [**H7**]) were further selected for MD simulations, this time containing 15LOX-2/Fer-1 complex and PEBP1 in the certain distance (~10 Å) to check whether Fer-1 in any of those three positions will affect PEBP1 binding to 15LOX-2. ENM analysis showed that Fer-1 bounded at *Site 2* significantly changes the allosteric movement that is gained upon PEBP1 binding to 15LOX (**Fig. 16C**, the low-frequency GNM mode profile), and the extensive MD data implied that Fer-1 affects PEBP1/15LOX-2 complex formation (**Fig. 16D**). PEBP1 was binding to 15LOX-2 to the previously predicted binding site (**Fig. 9A**) in the absence of Fer-1 (**Fig. 16D**, *top panel*) but not when Fer-1 was bound at *Site 2* (**Fig. 16D**, *bottom panel*). We observed two exceptions when PEBP1 bound at the predicted site, but in those cases, Fer-1 moved from the initial binding position (**Fig. 16D**, *bottom panel*, red and cyan PEBP1 and *Fig. S4* in [**H7**]). Our data implied that indeed Fer-1 does not affect 15LOX alone, but it effectively inhibits 15-HpETE-PE production by disrupting the 15LOX/PEBP1 complex formation.
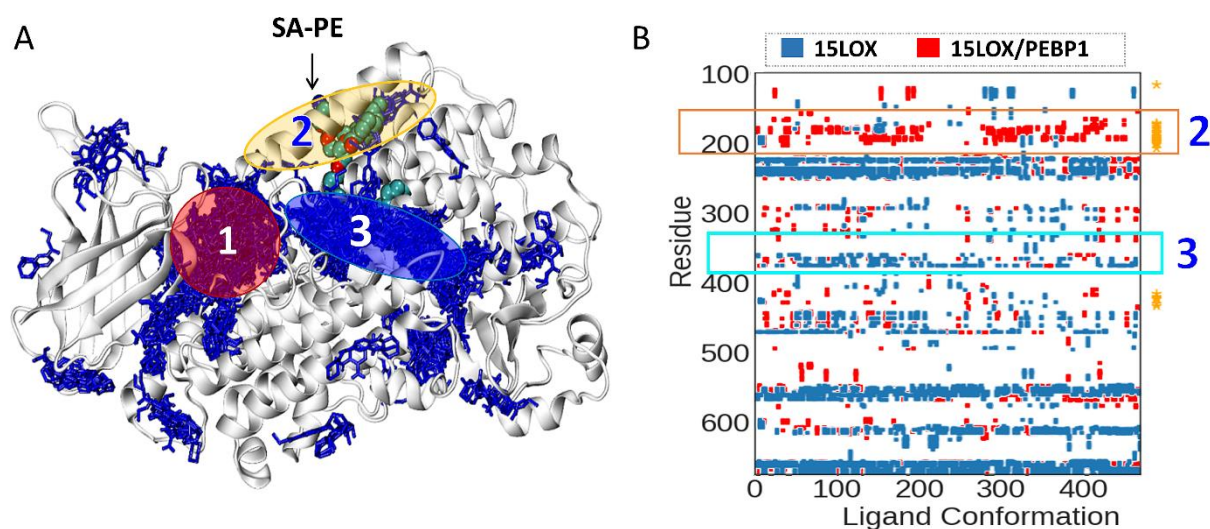

Figure 15. Fer-1 binding propensity observed in docking simulations with unbound 15LOX. *(A) Multiple binding poses of Fer-1 (blue sticks). Three sites are distinguished by their high propensities: Site 1 (pink circle) - an interface between the catalytic and β-barrel domains of 15LOX-2, Site 2 (yellow ellipse) – PEBP1-binding epitope of 15LOX, and Site 3 (blue ellipse) – 15LOX catalytic/orthosteric site. (B) Interaction map of 15LOX-2 residues interacting with Fer-1 observed in two sets of docking simulations, with the unbound (blue dots) and PEBP1-bound (red dots) forms of 15LOX-2. The orange box denotes Fer-1 binding residues at Site 2, and the cyan box points to the binding residues at Site 3. Orange stars denote the PEBP1-binding interface region. Source:* [**H7**].
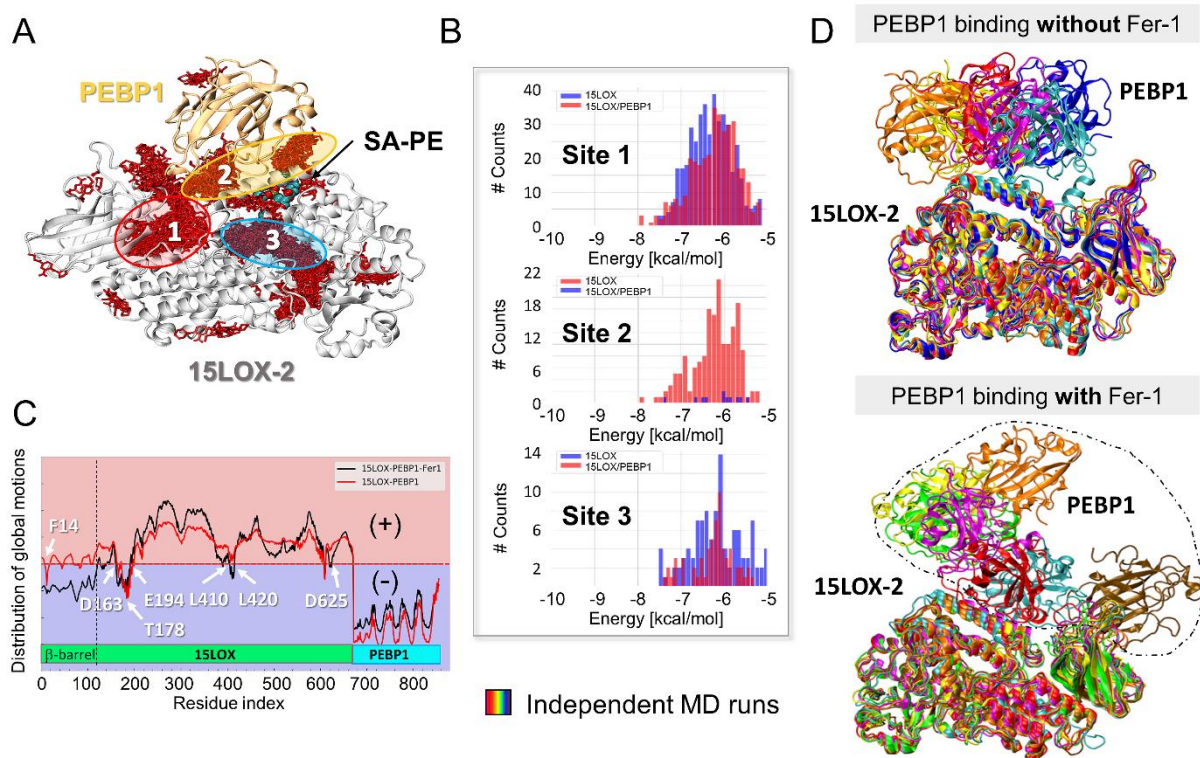
Figure 16. Effect of Fer-1 binding to the dynamics of 15LOX-2/PEBP1 complex. *(A) Multiple binding poses of Fer-1 (red sticks). Three sites, as in Fig. 15, are highlighted. Detailed interactions between Fer-1 and the human complex are shown in Fig. 15B (in red). (B) Histograms with the number of binding poses in each site, Site 1-3, for 15LOX-2 in bound/unbound form with PEBP1. (C) Comparison of global dynamics in GNM of 15LOX-2/PEBP1 complex in the presence (black-curve) and absence (red-curve) of Fer-1. Highlighted residues correspond to the hinge sites. (D) Final conformations from MD simulations of 15LOX-2/PEBP1 complexation without (top panel) and with Fer-1 bound to 15LOX-2 (bottom panel). Colors distinguish conformations from independent MD runs. Modified from* [**H7**].

Phospholipase iPLA2β (iii) Phospholipase A2 (PLA2) is a family of enzymes that can catalyze the cleavage of fatty acids by recognizing the sn-2 acyl chain of phospholipids and releasing arachidonic acid and lysophosphatidic acid, biologically active lipid mediators, that can affect numerous cellular events [130]. In [**H8**] study, we showed that the Ca^{2+}-independent phospholipase A2β (iPLA2β) could hydrolyze peroxidized SA-PE phospholipids, 15-HpETE-PE, generated by the human 15LOX/PEBP1 complex, thus eliminate the ferroptotic death signal and serve as the anti-ferroptotic guardian. This alternative 15-HpETE-PE-eliminating mechanism may be particularly important when thiol-driven defenses using the GPX-4 become insufficient (**Fig. 5**). Samples from a patient with a Parkinson's disease (PD)-associated mutation (R747W in iPLA2β), examined by the US collaborators, show selectively decreased 15-HpETE-PE-hydrolyzing activity, 15-HpETE-PE accumulation, and elevated sensitivity to ferroptosis [**H8**]. Herein, I performed extensive computational modeling using biophysical tools, which included successfully completing the following steps:

(i)   All-atom MD simulations for the membrane with a diverse number of phospholipids (9 types with the exact ratio as in the experiments, see *Extended Data Fig. 2* in [**H8**]), and including 15-HpETE-PE in order to obtain the peroxidized acyl chain of 15-HpETE-PE exposed to the membrane surface as proposed by the *Whisker model* (*Fig. 1c* in [**H8**])

[131]. The non-standard elements of the membrane, such as 15-HpETE-PE, required quantum calculations to obtain the geometry and partial charges for parametrization in the CHARMM force field.

(ii)   Preparation of the complete iPLA2β structure in a dimeric form since the crystallographic structure determined by our collaborators contained unsolved or partially unsolved fragments. To predict missing regions, I performed homology modeling using different available tools (*Fig. 1d* and *Extended Data Fig. 6* in [**H7**]). The entire model is available as the *Supplementary Material* of [**H7**] work and can be used by other scientists.

(iii)   I performed all-atom MD simulations to examine iPLA2β interactions with the membrane and 15-HpETE-PE molecules (prepared in (i)). The initial structure is shown in *Fig. 1d-e* in [**H7**], whereas the final interactions and differences between the native iPLA2β and its R747W mutant are displayed in *Fig. 2* in [**H8**]. Simulations included native iPLA2β structure [entire structure (catalytic domain with ankyrin repeats) or catalytic domain] and their mutants associated with PD (~0.5-1 mln atoms in MD systems).

My MD simulations visualized the ability of 15-HpETE-PE peroxidized acyl chain to migrate within the membrane surfaces (for the first time shown here the *Whisker model* of 15-HpETE-PE) than its counterpart in SA-PE (*Fig. 1c, Ext. Data Fig. 3b* and *Videos 1-3* in [**H8**]), i.e., having a higher probability to move closer to the iPLA2β surface and catalytic site (*Ext. Data Fig. 4a,b* in [**H8**]). It explains the experimentally observed higher iPLA2β activity toward 15-HpETE-PE compared to SA-PE. Quantitative analysis of the intrinsic dynamics of SA-PE in its oxidized and non-oxidized forms using the deuterium order parameters showed relatively higher ordering at the peroxidation site of 15-HpETE-PE than in SA-PE (*Ext. Data Fig. 5a,b* in [**H8**]). Moreover, simulations with/without R747W mutation provided detailed information about differences in interactions between protein structure and 15-HpETE-PE molecules (*Ext. Data Fig. 7* in [**H8**]) and about the molecular explanation of the lowered catalytic potency of R747W iPLA2β toward 15-HpETE-PE (*Fig. 2* in [**H8**]).

Summary. The publications presented as the habilitation achievement represents the collaborative work of a multidisciplinary team of scientist, both computational theoretical biophysicists and experimentalists, with complementary and valuable experience in scientific work. Each publication [**H1-H8**] brought a tremendous effort to each group, however, in final giving groundbreaking findings in the field of ferroptosis. As a computational biophysicist, I was using theoretical biophysical methods to provide computational modeling of the biological systems, often highly advanced and essential for understanding the molecular mechanisms described in the publications. My work provided a critical advancement in understanding molecular mechanisms of ferroptosis at the molecular level and was used for the improvements of the experimental studies of my collaborators. All the findings presented as the habilitation achievement were directed toward understanding the unknown molecular mechanisms of the ferroptotic cell death program and their mechanisms of inhibition, which is essential for developing rational intervention drugs associated with ferroptosis. The achievement presented above includes a description of the candidate's initiated, performed, and analyzed calculations. Results provided or prepared by Dr. I. Shrivastava or Dr. J. Krieger, by other members of the so-called "computational team" if any, were omitted in the description.

IV.3.4. Importance of the achievement and future studies

Importance. The results obtained in the proposed achievement have a significant impact on different scientific fields and disciplines, including biophysics, biochemistry, biology, and medicine. It can be seen by the number of citations given in a short time to each article of the habilitation achievement. Presented results are especially meaningful for the biomedical field because of their association with different diseases, e.g., major chronic degenerative diseases (Parkinson's, Alzheimer's), sepsis, asthma, cancers, pathology of cystic fibrosis, pneumonia, acute injuries of the brain, cardiovascular system, liver, kidneys, and other organs. Understanding the molecular basics of the mechanisms that lie under the ferroptotic cell death signal is essential for controlling this process and developing rational intervention drugs, i.e., inhibitors and methods for diseases associated with ferroptosis. This achievement brought significant scientific benefits in the form of understanding how the mechanisms of ferroptosis machinery work and how to block it. This knowledge provides a basis and advances general research in the field and shows the highly importance and indispensability of computational biophysics in the practical explanation of the fundamental biochemical process. This habilitation achievement offers additional information that might be used in drug discovery in clinical tests, for example, in the pathology of cystic fibrosis and pneumonia (pLoxA) or asthma (15LOX/PEBP1). The quality of research done by our team is the highest possible, and computationally, the candidate is using top-notch methods.

Future studies. My current and future studies are directed mainly toward the involvement of different lipid mediators in ferroptosis and other RCD programs and in the development of new computational tools which may benefit the broader research community. My plans include:

(i) **Examination of a di-arachidonoyl-PE possible role in the ferroptosis process.** This type of PUFA-PL contains two oxidizable chains instead of one like in SA-PE and has high specificity to the human 15LOX/PEBP1 complex. This is an ongoing project in collaboration with groups of Prof. V. Kagan and Prof. H. Bayır from the University of Pittsburgh, which may provide another missing puzzle of the ferroptosis machinery.

(ii) **Searching for new high-affinity inhibitors of pLoxA.** There is an urgent need for high-affinity pLoxA inhibitors which may serve as a means in the pathology of cystic fibrosis or pneumonia. I plan to explore the dynamics, selectivity toward different substrates, and mechanisms of actions of pLoxA to design new inhibitors. Application for funding which includes this topic, was submitted this year to the Polish National Science Centre (SONATA BIS program). It will include a collaboration between the groups of Prof. V. Kagan, Prof. H. Bayır, and Prof. S. Wenzel (head of the Asthma Institute at UPMC) from the University of Pittsburgh and a group of Dr. Ganesha Rai from the NIH National Center for Advancing Translational Sciences.

(iii) **Studying the role of the membrane for the human 15LOX-1/PEBP1 complex.** This is an ongoing project funded by the Polish National Science Centre (SONATA) under which a doctoral dissertation of Thiliban Manivarma will be prepared. In this project, we are examining the effect of the membrane on the 15LOX-1/PEBP1 complex.

(iv) **Examination of cyclooxygenase-2 dynamics and substrate specificity.** COX-2 is an enzyme that catalyzes the conversion of arachidonic acid (AA) to prostaglandin H2, an

important precursor of prostacyclin, which is expressed in inflammation. This protein will be a subject of the next studies in collaboration with experimentalist groups of Prof. V. Kagan and Prof. H. Bayır. We will study substrate specificity toward different lipids.

(v) **Cytochrome c interactions with cardiolipin molecules and its different variants.** This is an ongoing project in collaboration with Prof. I. Bahar from Stony Brook University (NY, USA) and Prof. Patrick van der Wel from the University of Groningen (Netherlands), which regards lipid interactions with Cyt *c* and its role in severe diseases.

(vi) **Development of a computational tool for the assessment of inhibitor binding sites for the protein dynamics.** Currently, I am working on the ProDy [132] module that will help to estimate potential intermolecular interactions within protein structure or between protein and ligand (**Fig. 17A**). This approach will provide interaction-rich regions which will be combined with information obtained from ENMs (e.g., hinge sites, allosteric sites, cross-correlation and hitting time, **Fig. 17B**), and sequence conservation (based on the Pfam [133] data, **Fig. 17C**) to evaluate the influence of ligand/protein binding site on the protein dynamics. Consolidation of those approaches enables the broader community to explore physical interactions within biological structures combined with sequence conservation and coarse-grained-associated knowledge about collective dynamics might be critical in choosing the most effective inhibitor and their binding spots. This project is implemented in collaboration with Dr. J. Krieger from the Universidad Autónoma de Madrid, Spain and Prof. I. Bahar from the Stony Brook University, New York, USA.
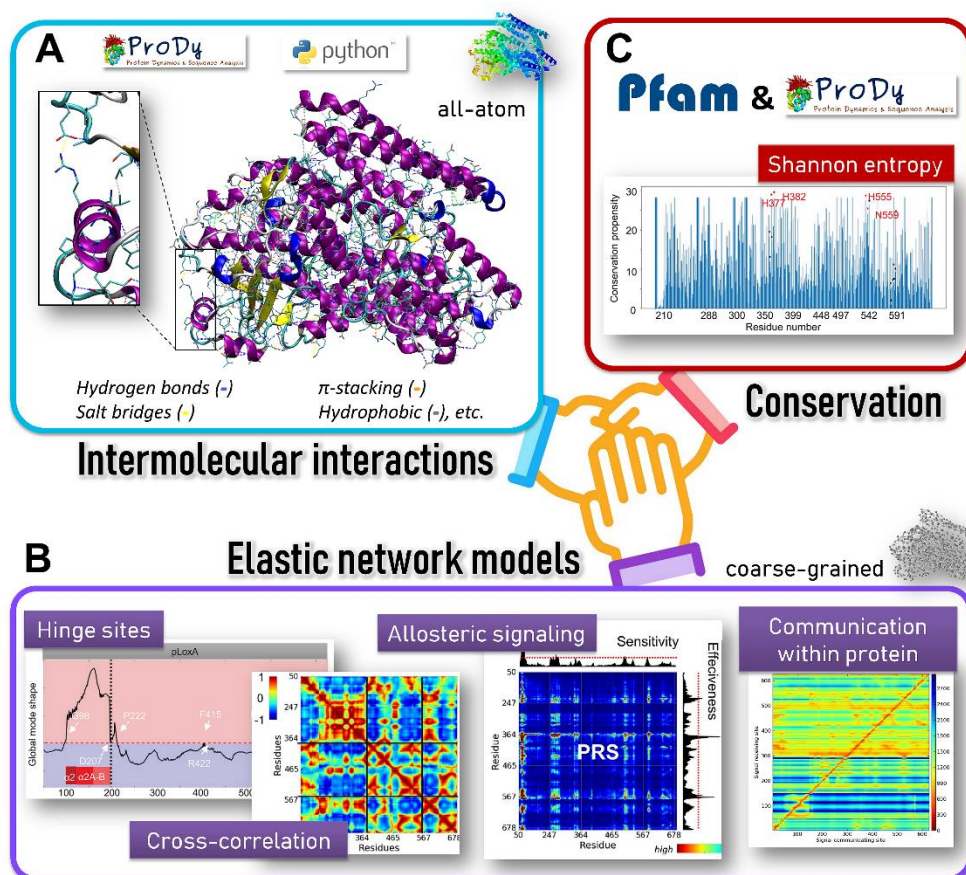

Figure 17. *Flow chart describing how the new tool will operate with the usage of (A) intermolecular interactions (B) elastic network models (ENMs), and (C) sequence conservation.*

IV.3.5. Other scientific achievements

For the past years, I have been involved in several side projects devoted to investigating protein's different features, e.g., protein dynamics, nanomechanics, and substrate specificity toward protein structures involved in different diseases. The topics described below (*Topic 1-4*) are relatively distant thematically from the achievement; therefore, they are not included in the habilitation achievement. However, some of them become independent threads that are evolving and becoming an equally important field of interest for the candidate, such as deciphering mechanisms of other RCD programs (*Topic 1*) or developing new tools for the computational biophysics field (*Topic 3*).

Topic 1: **Lipids mediators in other RCD programs**. For the past two decades, we could observe a growing number of RCD programs and their implications in human pathologies. RCDs are usually highly orchestrated processes involving tightly structured signaling cascades and strictly defined mechanisms. The habilitation achievement is focused on the ferroptosis mechanism; however, I was also involved in the investigation of two other RCD programs – apoptosis [**A1**] (collaboration with Prof. P. Wel, Prof. V. Kagan, and a few more groups) and autophagy [**A2**] (collaboration with Prof. M. Arditi and Prof. I. Bahar). For those two independent projects, I performed extensive all-atom MD simulations in the presence of a phospholipid membrane to study cytochrome *c* (Cyt *c*) [**A1**] and pro-interleukin-1α (IL-1α) [**A2**] interactions with cardiolipin (CL) molecules or its variant (e.g., mono-lyso-CL (MLCL)). My modeling for the [**A1**] study provided evidence that MLCL, which is accumulating in the rare genetic disorder called the Barth syndrome, forms an anomalous complex with Cyt *c* and causes PUFA phospholipid peroxidation, which may be the primary mechanism of this disorder. I showed which Cyt *c* residues are involved in the initial and stable interactions with the membrane, what conformational change is happening upon MLCL binding, and how the Cyt *c* interacts with IOA (imidazole oleic acid) inhibitor. All my results correspond well to the lipidomics and solid-state NMR observations provided by my collaborators. In the [**A2**] study, I identified a pro-IL-1α binding motif with CL molecules from the membrane using MD simulations. My experimental collaborators confirmed my observations in mutagenesis studies. Moreover, a similar binding motif I found in microtubule-associated proteins 1A/1B light chain 3B (LC3β, sequence alignment and screening of similar motif), a central protein in autophagy. Thus, we could imply that the binding of pro-IL-1α to CL may interrupt CL-LC3β-dependent mitophagy, which is an important finding in NLRP3 inflammasome-associated diseases.

Topic 2: **Nanomechanics of modular proteins using force-inducted approaches**. Most of the proteins have strictly defined native structures. Modifications to its composition or conformation may lead to severe defects. However, native structure of some proteins often naturally undergoes significant conformational changes, for example, due to mechanical stress. In such cases, mechanical stability plays an important role and directly impacts many biological processes, e.g., muscle work or translocation of molecules through the cell membrane. These mechanisms are conditioned by specific places and the method of applying external forces to proteins. Thus, in the past years, there has been a lot of interest in methods for studying the nanomechanical properties of single molecules. Using two complementary methods, computational (steered molecular dynamics, SMD) and experimental (single molecule force

spectroscopy, SMFS, AFM), I performed studies in which I applied an external force to protein structures to obtain a force spectra profile of their mechanical behavior. My experience in that field was gained during my doctoral studies and used here to extract the characteristic of protein's unfolding pathways, a force that is needed to induce a conformational change in each domain, etc. Two modular proteins were the subjects of those studies: contactin 4 [**A4**] and reelin [**A3**] (the experimental part for reelin was performed by Dr. J. Strzelecki NCU).

Topic 3: **Development of new methods and their deployment to protein structures**. Despite the biophysical and biochemical aspects of my scientific work, I was also involved in projects developing new computational tools and methods to analyze protein dynamics [**A4-A6**]. Because I had an experience in experimental and computational force spectroscopy (steered MD method and SMFS technique described in *Topic 2*), my first task as a post-doc in the group of Prof. I. Bahar was to implement to the ProDy API (introduced by Bahar Lab in 2011, http://prody.csb.pitt.edu/, >2,3 mln downloads) a new module called *MechStiff* for determining the weak and strong pairs of interactions depending on the direction of the external force and the sites that are subjected to perturbation. *MechStiff* uses the coarse-grained ANM concept, and it helps in the identification of the anisotropic response of the structure to external perturbations. After implementation, I used this tool to provide information about the composition of effective spring constant in the presence of external force for each contactin 4 module [**A4**]. I was also involved in the project that introduced the *CryoDy* module, which calculates the dynamics of protein complexes resolved by cryo-EM by approximating the density maps with pseudo atoms [**A5**], where I was performing ANM calculations of various chaperone TRiC/CCT cryo-EM structures which were a subject of this project. The involvement in developing ProDy modules was summarized in [**A6**] work, where we introduced new modules/methods implemented in ProDy in the past ten years.

Topic 4: **Insect-repellent studies**. Mosquitoes are one of the most dangerous animals on Earth, transmitting diseases that are killing nearly a million people each year, thus being one of the major causes of human mortality. The primary protection against mosquitoes are repellants, i.e., chemical compounds that repel insects, mainly by affecting their extremely sensitive sense of smell. The most commonly used chemicals containing DEET gradually lose their activity due to the progressive resistance of mosquitoes. Consequently, there is an important need to create new strategies to fight against them. Muscarinic receptors are a family of transmembrane G protein-coupled receptors (GPCRs) which plays a vital role in the nervous systems of humans and mosquitoes [134, 135]. In this project, I was performing molecular docking calculations to predict plausible DEET binding sites in M1 and M3 acetylcholine receptors at allosteric and orthostatic sites (*Fig. 4D-E* and *Fig. 5* in [**A7**], and details in *Table S4*). That information was further used to test different types of repellents and to compare their binding sites and affinities toward those receptors (*Fig. 4, Fig. 7,* and *Fig. S1* in [**A8**]).

References

Articles included in the habilitation achievement

[H1] *PEBP1 wardens ferroptosis by enabling lipoxygenase generation of lipid death signals*
S. Wenzel, Y. Tyurina, J. Zhao, C. Croix, H. Dar, G. Mao, V. Tyurin, T. Anthonymuthu,
A. Kapralov, A. Amoscato, **K. Mikulska-Ruminska**, I. Shrivastava, E. Kenny, Q. Yang,
J. Rosenbaum, L. Sparvero, D. Emlet, X. Wen, Y. Minami, F. Qu, S. Watkins, T. Holman,
A. VanDemark, J. Kellum, I. Bahar, H. Bayır, V. Kagan, *Cell*, 171 (2017) 628-641.

[H2] *Empowerment of 15-Lipoxygenase Catalytic Competence in Selective Oxidation of Membrane ETE-PE to Ferroptotic Death Signals*, *HpETE-PE,* T. Anthonymuthu, E. Kenny,
I. Shrivastava, Y. Tyurina, Z. Hier, H. Ting, H. Dar, V. A. Tyurin, A. Nesterova, A. Amoscato,
K. Mikulska-Ruminska, J. Rosenbaum, G. Mao, J. Zhao, M. Conrad, J. Kellum, S. Wenzel,
A. VanDemark, I. Bahar, V. Kagan, H. Bayir, *J. Am. Chem. Soc.*, 140 (2018) 17835-17839.

[H3] *Pseudomonas aeruginosa utilizes host polyunsaturated phosphatidylethanolamines to trigger theft-ferroptosis in bronchial epithelium*, H. Dar, Y. Tyurina, **K. Mikulska-Ruminska**,
I. Shrivastava, H. Ting, V. Tyurin, J. Krieger, C. Croix, S. Watkins, E. Bayir, G. Mao,
C. Armbruster, A. Kapralov, H. Wang, M. Parsek, T. Anthonymuthu, A. Ogunsola, B. Flitter,
C. Freedman, J. Gaston, T. Holman, J. Pilewski, J. Greenberger, R. Mallampalli, Y. Doi,
J. Lee, I. Bahar, J. Bomberger, H. Bayır, V. Kagan, *J. Clin. Invest.*, 128 (2018) 4639-4653.

[H4] *Characterization of Differential Dynamics, Specificity, and Allostery of Lipoxygenase Family Members*, **K. Mikulska-Ruminska**, I. Shrivastava, J. Krieger, S. Zhang, H. Li, H. Bayır, S.
Wenzel, A. VanDemark, V. Kagan, I. Bahar, *J. Chem. Inform. Model.*, 59 (2019) 2496-2508.

[H5] *Redox Lipid Reprogramming Commands Susceptibility of Macrophages and Microglia to Ferroptotic Death*, A. Kapralov, Q. Yang, H. Dar, Y. Tyurina, T. Anthonymuthu, R. Kim,
C. Croix, **K. Mikulska-Ruminska**, B. Liu, I. Shrivastava, V. Tyurin, H. Ting, Y. Gao,
R. Domingues, D. Stoyanovsky, R. Mallampalli, I. Bahar, D. Gabrilovich, H. Bayir, V. Kagan,
Nature Chem. Biol., 3 (2020) 278-290.

[H6] *NO$^\bullet$ Represses the Oxygenation of Arachidonoyl PE by 15LOX/PEBP1: Mechanism and Role in Ferroptosis*, **K. Mikulska-Ruminska**, T. Anthonymuthu, A. Levkina, I. Shrivastava,
A. Kapralov, H. Bayır, V. Kagan, I. Bahar, *Inter. J. Mol. Sci.,* 22 (2021) 5253.

[H7] *Resolving the paradox of ferroptotic cell death: Ferrostatin-1 binds to 15LOX/PEBP1 complex, suppresses generation of Peroxidized ETE-PE, and protects against ferroptosis*
T. Anthonymuthu, Y. Tyurina, W. Sun, **K. Mikulska-Ruminska**, I. Shrivastava, V. Tyurin,
F. Cinemre, H. Dar, A. VanDemark, T. Holman, Y. Sadovsky, B. Stockwell, R. He, I. Bahar,
H. Bayır, V. Kagan, *Redox Biol.*, 38 (2021) 101744.

[H8] *Phospholipase iPLA2b Averts Ferroptosis by Eliminating Death Signal, 15HpETE-PE: Relevance to Parkinson's Disease,* W. Sun, V. Tyurin, **K. Mikulska-Ruminska**,
I. Shrivastava, B. Liu, Y. Zhai, M. Pan, H. Gong, D. Lu, J. Sun, W. Duan, S. Korolev,
A. Abramov, P. Angelova, I. Miller, O. Beharier, G. Mao, H. Dar, A. Kapralov, T. Hastings,
J. Greenamyre, C. Chu, Y. Sadovsky, I. Bahar, H. Bayır, Y. Tyurina, R. He, V. Kagan,
Nature Chem. Biol., 17 (2021) 1-12.

One should note that the studies implement a multidisciplinary approach and represent a collaborative work of a multidisciplinary team of scientists with complementary expertise in structural biophysics, biochemistry, crystallography, computational modeling, mass spectroscopy, lipidomics, imagining, cell biology, and involve >10 institutions from the University of Pittsburgh, Nicolaus Copernicus University, UPMC Hospital and a few occasional collaborations on particular parts of the project, for example, collaboration with Prof. Brent Stockwell – a scientist who proposed for the first time the concept of ferroptosis in 2012.

Other works by the candidate

[A1] *Recruitment of pro-IL-1a to Mitochondrial Cardiolipin, via shared LC3 Binding Domain, Drives Nlrp3 Activation and Inhibits Mitophagy,* J. Dagvadorj, **K. Mikulska-Ruminska**, G. Tumurkhuu, R. Ratsimandresy, J. Carriere, A. Andres, Y. Song, S. Chen, M. Lane, A. Dorfleutner, R. Gottlieb, C. Stehlik, S. Cassel, F. Sutterwala, I. Bahar, T. Crother, M. Arditi, *Proc. Nat. Acad. Sci.* (*PNAS*), 118 (2021).

[A2] *Anomalous* peroxidase is the primary pathogenic target in Barth syndrome, V. Kagan, Y. Tyurina, **K. Mikulska-Ruminska**, D. Damschroder, A. Lasorsa, A. Kapralov, V. Tyurin, A. Amoscato, S. Samovich, H. Dar, A. Ramim, P. Lazcano, J. Ji, M. Schmidtke, G. Vladimirov, M. Artyukhova, P. Rampratap, L. Cole, A. Niyatie, E. Baker, J. Peterson, G. Hatch, J. Atkinson, B. Kühn, R. Wessells, P. Wel, I. Bahar, H. Bayir, M. Greenberg, Nature Metabolism (2022, *during major revision*).

[A3] *Dynamics, nanomechanics and signal transduction in reelin repeats*, **K. Mikulska-Ruminska**, J. Strzelecki, W. Nowak, *Sci. Rep.,* 9 (2019) 1-13.

[A4] *Nanomechanical unfolding scenarios of multidomain neuronal cell adhesion protein contactin revealed by single molecule AFM and SMD*, **K. Mikulska-Ruminska**, A. Kulik, C. Benadiba, I. Bahar, G. Dietler, W. Nowak, Sci. Rep., 7 (2017) 8852.

[A5] *Sequential Allosteric Dynamics of Chaperonin TRiC/CCT Elucidated by Network Analysis of Cryo-EM Maps*, Y. Zhang, J. Krieger, **K. Mikulska-Ruminska**, B. Kaynak, C. Sorzano, J. Carazo, A. Horovitz, J. Xing, I. Bahar, *Prog. Biophys. Mol. Biol.,* 160 (2020) 104-120.

[A6] *ProDy 2.0: Increased scale and scope after 10 years of protein dynamics modelling with Python,* S. Zhang, J. Krieger, Y. Zhang, C. Kaya, B. Kaynak, **K. Mikulska-Ruminska**, P. Doruker, H. Li, I. Bahar, *Bioinformatics* (2021) 1-3, DOI: 10.1093/bioinformatics/btab18

[A7] *The repellent DEET potentiates carbamate effects via insect muscarinic receptor interactions: An alternative strategy to control insect vector-borne diseases*, A. Abdella, M. Stankiewicz, **K. Mikulska**, W. Nowak, C. Pennetier, M. Goulu, C. Fruchart-Gaillard, P. Licznar, V. Apaire-Marchais, O. List, V. Corbel, D. Servent, B. Lapied, *PLOS ONE,* 10 (2015) e0126406.

[A8] *Orthosteric muscarinic receptor activation by the insect repellent IR3535 opens new prospects in insecticide-based vector control*, E. Moreau, **K. Mikulska-Ruminska**, M. Goulu, S. Perrier, C. Deshayes1, M. Stankiewicz, V. Apaire-Marchais, W. Nowak, B. Lapied, *Sci. Rep.*, 10 (2020) 1-15.

References by other authors

1. Santoro, M.M., *The antioxidant role of non-mitochondrial CoQ10: mystery solved!* Cell metabolism, 2020. **31**(1): p. 13-15.
2. Li, J., et al., *Ferroptosis: past, present and future.* Cell death & disease, 2020. **11**(2): p. 1-13.
3. Bianconi, E., et al., *An estimation of the number of cells in the human body.* Annals of human biology, 2013. **40**(6): p. 463-471.
4. Lobo, N.A., et al., *The biology of cancer stem cells.* Annu. Rev. Cell Dev. Biol., 2007. **23**: p. 675-699.
5. Harley, C.B., et al. *Telomerase, cell immortality, and cancer*. in *Cold Spring Harbor symposia on quantitative biology*. 1994. Cold Spring Harbor Laboratory Press.
6. Kim-Campbell, N., H. Gomez, and H. Bayir, *Cell death pathways: apoptosis and regulated necrosis*, in *Critical care nephrology*. 2019, Elsevier. p. 113-121. e2.
7. Galluzzi, L., et al., *Essential versus accessory aspects of cell death: recommendations of the NCCD 2015.* Cell Death & Differentiation, 2015. **22**(1): p. 58-73.
8. Cao, J.Y. and S.J. Dixon, *Mechanisms of ferroptosis.* Cellular and Molecular Life Sciences, 2016. **73**(11): p. 2195-2209.
9. Gao, M., et al., *Ferroptosis is an autophagic cell death process.* Cell research, 2016. **26**(9): p. 1021-1032.
10. Capelletti, M.M., et al., *Ferroptosis in liver diseases: an overview.* International journal of molecular sciences, 2020. **21**(14): p. 4908.
11. Dixon, S.J., et al., *Ferroptosis: an iron-dependent form of nonapoptotic cell death.* Cell, 2012. **149**(5): p. 1060-1072.

12. Tang, D., et al., *Ferroptosis: molecular mechanisms and health implications.* Cell research, 2021. **31**(2): p. 107-125.

13. Bao, W.-D., et al., *Loss of ferroportin induces memory impairment by promoting ferroptosis in Alzheimer's disease.* Cell Death & Differentiation, 2021. **28**(5): p. 1548-1562.

14. Yan, N. and J. Zhang, *Iron metabolism, ferroptosis, and the links with Alzheimer's disease.* Frontiers in neuroscience, 2020. **13**: p. 1443.

15. Guiney, S.J., et al., *Ferroptosis and cell death mechanisms in Parkinson's disease.* Neurochemistry international, 2017. **104**: p. 34-48.

16. Sun, W.-Y., et al., *Phospholipase iPLA 2 β averts ferroptosis by eliminating a redox lipid death signal.* Nature Chem. Biol., 2021: p. 1-12.

17. Yang, W.S. and B.R. Stockwell, *Ferroptosis: death by lipid peroxidation.* Trends in cell biology, 2016. **26**(3): p. 165-176.

18. Miotto, G., et al., *Insight into the mechanism of ferroptosis inhibition by ferrostatin-1.* Redox Biol., 2020. **28**: p. 101328.

19. Lu, B., et al., *The role of ferroptosis in cancer development and treatment response.* Front. Pharmacol,, 2018. **8**: p. 992.

20. Xu, T., et al., *Molecular mechanisms of ferroptosis and its role in cancer therapy.* Journal of cellular and molecular medicine, 2019. **23**(8): p. 4900-4912.

21. Shen, Z., et al., *Emerging strategies of cancer therapy based on ferroptosis.* Advanced Materials, 2018. **30**(12): p. 1704007.

22. Liang, C., et al., *Recent progress in ferroptosis inducers for cancer therapy.* Advanced materials, 2019. **31**(51): p. 1904197.

23. Yang, M. and C.L. Lai, *SARS-CoV-2 infection: can ferroptosis be a potential treatment target for multiple organ involvement?* Cell death discovery, 2020. **6**(1): p. 1-6.

24. Fratta Pasini, A.M., et al., *Is Ferroptosis a Key Component of the Process Leading to Multiorgan Damage in COVID-19?* Antioxidants, 2021. **10**(11): p. 1677.

25. Tavakol, S. and A.M. Seifalian, *Vitamin E at a high dose as an anti-ferroptosis drug and not just a supplement for COVID-19 treatment.* Biotechnology and applied biochemistry, 2021.

26. Singh, Y., et al., *SARS CoV-2 aggravates cellular metabolism mediated complications in COVID-19 infection.* Dermatologic therapy, 2020. **33**(6): p. e13871.

27. Wenzel, S.E., et al., *PEBP1 Wardens Ferroptosis by Enabling Lipoxygenase Generation of Lipid Death Signals.* Cell, 2017. **171**(3): p. 628-641. e26.

28. Stockwell, B.R., et al., *Ferroptosis: a regulated cell death nexus linking metabolism, redox biology, and disease.* Cell, 2017. **171**(2): p. 273-285.

29. Conrad, M., et al., *Regulation of lipid peroxidation and ferroptosis in diverse species.* Genes & development, 2018. **32**(9-10): p. 602-619.

30. Konstorum, A., et al., *Systems biology of ferroptosis: A modeling approach.* Journal of theoretical biology, 2020. **493**: p. 110222.

31. Yang, W.S., et al., *Peroxidation of polyunsaturated fatty acids by lipoxygenases drives ferroptosis.* Proceedings of the National Academy of Sciences, 2016. **113**(34): p. E4966-E4975.

32. Gill, I. and R. Valivety, *Polyunsaturated fatty acids, part 1: occurrence, biological activities and applications.* Trends in biotechnology, 1997. **15**(10): p. 401-409.

33. Bazinet, R.P. and S. Layé, *Polyunsaturated fatty acids and their metabolites in brain function and disease.* Nature Reviews Neuroscience, 2014. **15**(12): p. 771-785.

34. Porter, N.A., et al., *The autoxidation of arachidonic acid: formation of the proposed SRS-A intermediate.* Biochemical and biophysical research communications, 1979. **89**(4): p. 1058-1064.

35. Rouzer, C.A. and L.J. Marnett, *Mechanism of free radical oxygenation of polyunsaturated fatty acids by cyclooxygenases.* Chemical reviews, 2003. **103**(6): p. 2239-2304.

36. Yan, H.-f., et al., *Ferroptosis: mechanisms and links with diseases.* Signal transduction and targeted therapy, 2021. **6**(1): p. 1-16.

37. Piperno, A., S. Pelucchi, and R. Mariani, *Inherited iron overload disorders.* Translational gastroenterology and hepatology, 2020. **5**.

38. Han, C., et al., *Ferroptosis and its potential role in human diseases.* Frontiers in pharmacology, 2020. **11**: p. 239.

39. Forcina, G.C. and S.J. Dixon, *GPX4 at the crossroads of lipid homeostasis and ferroptosis.* Proteomics, 2019. **19**(18): p. 1800311.

40. Winterbourn, C.C., *Toxicity of iron and hydrogen peroxide: the Fenton reaction.* Toxicology letters, 1995. **82**: p. 969-974.

41. Hassannia, B., P. Vandenabeele, and T.V. Berghe, *Targeting ferroptosis to iron out cancer.* Cancer cell, 2019. **35**(6): p. 830-849.

42. Knutson, M.D., *Steap proteins: implications for iron and copper metabolism.* Nutrition reviews, 2007. **65**(7): p. 335-340.

43. Sun, X., et al., *HSPB1 as a novel regulator of ferroptotic cancer cell death.* Oncogene, 2015. **34**(45): p. 5617-5625.

44. Kerins, M.J. and A. Ooi, *The roles of NRF2 in modulating cellular iron homeostasis.* Antioxidants & redox signaling, 2018. **29**(17): p. 1756-1773.

45. Bellelli, R., et al., *NCOA4 deficiency impairs systemic iron homeostasis.* Cell reports, 2016. **14**(3): p. 411-421.

46. Straub, K.L., M. Benz, and B. Schink, *Iron metabolism in anoxic environments at near neutral pH.* FEMS microbiology ecology, 2001. **34**(3): p. 181-186.

47. Feig, A.L. and S.J. Lippard, *Reactions of non-heme iron (II) centers with dioxygen in biology and chemistry.* Chemical Reviews, 1994. **94**(3): p. 759-805.

48. Aisen, P., C. Enns, and M. Wessling-Resnick, *Chemistry and biology of eukaryotic iron metabolism.* The international journal of biochemistry & cell biology, 2001. **33**(10): p. 940-959.

49. Reichert, C.O., et al., *Ferroptosis mechanisms involved in neurodegenerative diseases.* International Journal of Molecular Sciences, 2020. **21**(22): p. 8765.

50. Shintoku, R., et al., *Lipoxygenase-mediated generation of lipid peroxides enhances ferroptosis induced by erastin and RSL3.* Cancer science, 2017. **108**(11): p. 2187-2194.

51. Singh, N.K. and G.N. Rao, *Emerging role of 12/15-Lipoxygenase (ALOX15) in human pathologies.* Progress in lipid research, 2019. **73**: p. 28-45.

52. Ackermann, J.A., et al., *The double-edged role of 12/15-lipoxygenase during inflammation and immunity.* Biochimica et Biophysica Acta (BBA)-Molecular and Cell Biology of Lipids, 2017. **1862**(4): p. 371-381.

53. Saura, P., et al., *Computational insight into the catalytic implication of head/tail-first orientation of arachidonic acid in human 5-lipoxygenase: consequences for the positional specificity of oxygenation.* Physical Chemistry Chemical Physics, 2016. **18**(33): p. 23017-23035.

54. Kagan, V.E., et al., *Oxidized arachidonic and adrenic PEs navigate cells to ferroptosis.* Nature Chem. Biol., 2017. **13**(1): p. 81-90.

55. Kuhn, H., S. Banthiya, and K. Van Leyen, *Mammalian lipoxygenases and their biological relevance.* Biochimica et Biophysica Acta (BBA)-Molecular and Cell Biology of Lipids, 2015. **1851**(4): p. 308-330.

56. Ou, Y., et al., *Activation of SAT1 engages polyamine metabolism with p53-mediated ferroptotic responses.* Proceedings of the National Academy of Sciences, 2016. **113**(44): p. E6806-E6812.

57. Green, D.R., et al., *Immunogenic and tolerogenic cell death.* Nature Reviews Immunology, 2009. **9**(5): p. 353-363.

58. Green, D.R., L. Galluzzi, and G. Kroemer, *Metabolic control of cell death.* Science, 2014. **345**(6203): p. 1250256.

59. Ursini, F., et al., *Purification from pig liver of a protein which protects liposomes and biomembranes from peroxidative degradation and exhibits glutathione peroxidase activity on phosphatidylcholine hydroperoxides.* Biochimica et Biophysica Acta (BBA)-Lipids and Lipid Metabolism, 1982. **710**(2): p. 197-211.

60. Ursini, F., M. Maiorino, and C. Gregolin, *The selenoenzyme phospholipid hydroperoxide glutathione peroxidase.* Biochimica et Biophysica Acta (BBA)-General Subjects, 1985. **839**(1): p. 62-70.

61. Margis, R., et al., *Glutathione peroxidase family–an evolutionary overview.* The FEBS journal, 2008. **275**(15): p. 3959-3970.

62. Brigelius-Flohé, R. and M. Maiorino, *Glutathione peroxidases.* Biochimica et Biophysica Acta (BBA)-General Subjects, 2013. **1830**(5): p. 3289-3303.

63. Wu, G., et al., *Glutathione metabolism and its implications for health.* The Journal of nutrition, 2004. **134**(3): p. 489-492.

64. Carlberg, I. and B. Mannervik, *[59] Glutathione reductase*, in *Methods in enzymology*. 1985, Elsevier. p. 484-490.

65. Dolphin, D., R. Poulson, and O. Avramovic, *Glutathione: chemical, biochemical, and medical aspects*. Vol. 3. 1989: Wiley New York.

66. Wu, X., et al., *Ferroptosis as a novel therapeutic target for cardiovascular disease.* Theranostics, 2021. **11**(7): p. 3052.

67. Halprin, K.M. and A. Ohkawara, *The measurement of glutathione in human epidermis using glutathione reductase.* J. Invest. Dermatol, 1967. **48**(2): p. 149.

68. Pastore, A., et al., *Determination of blood total, reduced, and oxidized glutathione in pediatric subjects.* Clinical chemistry, 2001. **47**(8): p. 1467-1469.

69. Dong, X., et al., *Global Characteristics and Trends in Research on Ferroptosis: A Data-Driven Bibliometric Study.* Oxidative Medicine and Cellular Longevity, 2022. **2022**.

70. Bersuker, K., et al., *The CoQ oxidoreductase FSP1 acts parallel to GPX4 to inhibit ferroptosis.* Nature, 2019: p. 1-1.

71. Doll, S., et al., *FSP1 is a glutathione-independent ferroptosis suppressor.* Nature, 2019: p. 1-1.

72. Crane, F.L., *Discovery of ubiquinone (coenzyme Q) and an overview of function.* Mitochondrion, 2007. **7**: p. S2-S7.

73. Frei, B., M.C. Kim, and B.N. Ames, *Ubiquinol-10 is an effective lipid-soluble antioxidant at physiological concentrations.* Proceedings of the National Academy of Sciences, 1990. **87**(12): p. 4879-4883.

74. Becker, O.M., et al., *Computational biochemistry and biophysics.* 2001: CRC Press.

75. Samish, I., P.E. Bourne, and R.J. Najmanovich, *Achievements and challenges in structural bioinformatics and computational biophysics.* Bioinformatics, 2015. **31**(1): p. 146-150.

76. Pagadala, N.S., K. Syed, and J. Tuszynski, *Software for molecular docking: a review.* Biophysical reviews, 2017. **9**(2): p. 91-102.

77. Yuriev, E. and P.A. Ramsland, *Latest developments in molecular docking: 2010–2011 in review.* Journal of Molecular Recognition, 2013. **26**(5): p. 215-239.

78. Koes, D.R., M.P. Baumgartner, and C.J. Camacho, *Lessons learned in empirical scoring with smina from the CSAR 2011 benchmarking exercise.* J. Chem. Inf. Mod., 2013. **53**(8): p. 1893-1904.

79. Tovchigrechko, A. and I.A. Vakser, *GRAMM-X public web server for protein–protein docking.* Nucl Acids Res, 2006. **34**: p. W310-W314.

80. Warshel, A. and M. Levitt, *Theoretical studies of enzymic reactions: dielectric, electrostatic and steric stabilization of the carbonium ion in the reaction of lysozyme.* Journal of molecular biology, 1976. **103**(2): p. 227-249.

81. McCammon, J.A., B.R. Gelin, and M. Karplus, *Dynamics of folded proteins.* Nature, 1977. **267**: p. 585-590.

82. Hospital, A., et al., *Molecular dynamics simulations: advances and applications.* Advances and applications in bioinformatics and chemistry: AABC, 2015. **8**: p. 37.

83. Karplus, M. and G.A. Petsko, *Molecular dynamics simulations in biology.* Nature, 1990. **347**(6294): p. 631-639.

84. Berman, H.M., et al., *The protein data bank.* Nucl. Aci. Res., 2000. **28**(1): p. 235-242.

85. Durrant, J.D. and J.A. McCammon, *Molecular dynamics simulations and drug discovery.* BMC biology, 2011. **9**(1): p. 71.

86. Verlet, L., *Computer" experiments" on classical fluids. I. Thermodynamical properties of Lennard-Jones molecules.* Physical review, 1967. **159**(1): p. 98.

87. Karplus, M. and J.A. McCammon, *Molecular dynamics simulations of biomolecules.* Nature Struct. Mol. Biol., 2002. **9**(9): p. 646-652.

88. Allen, M.P., *Introduction to molecular dynamics simulation.* Computational Soft Matter: From Synthetic Polymers to Proteins, 2004. **23**: p. 1-28.

89. Kundu, S., et al., *Dynamics of proteins in crystals: comparison of experiment with simple models.* Biophysical journal, 2002. **83**(2): p. 723-732.

90. Tama, F. and Y.-H. Sanejouand, *Conformational change of proteins arising from normal mode calculations.* Protein engineering, 2001. **14**(1): p. 1-6.

91. Herguedas, B., et al., *Structure and organization of heteromeric AMPA-type glutamate receptors.* Science, 2016. **352**(6285): p. aad3873.

92. Kmiecik, S., et al., *Modeling of protein structural flexibility and large-scale dynamics: Coarse-grained simulations and elastic network models.* International journal of molecular sciences, 2018. **19**(11): p. 3496.

93. Yang, L., G. Song, and R.L. Jernigan, *How well can we understand large-scale protein motions using normal modes of elastic network models?* Biophysical journal, 2007. **93**(3): p. 920-929.

94. Atilgan, A., et al., *Anisotropy of fluctuation dynamics of proteins with an elastic network model.* Biophys. J., 2001. **80**(1): p. 505-515.

95. Bahar, I., A.R. Atilgan, and B. Erman, *Direct evaluation of thermal fluctuations in proteins using a single-parameter harmonic potential.* Folding and Design, 1997. **2**(3): p. 173-181.

96. Atilgan, A., et al., *Anisotropy of fluctuation dynamics of proteins with an elastic network model.* Biophysical Journal, 2001. **80**(1): p. 505-515.

97. Flory, P.J., *Statistical thermodynamics of random networks.* Proceedings of the Royal Society of London. A. Mathematical and Physical Sciences, 1976. **351**(1666): p. 351-380.

98. Rouse Jr, P.E., *A theory of the linear viscoelastic properties of dilute solutions of coiling polymers.* The Journal of Chemical Physics, 1953. **21**(7): p. 1272-1280.

99. Eyal, E., L.-W. Yang, and I. Bahar, *Anisotropic network model: systematic evaluation and a new web interface.* Bioinformatics, 2006. **22**(21): p. 2619-2627.

100. Haliloglu, T., I. Bahar, and B. Erman, *Gaussian dynamics of folded proteins.* Phys. Rev. Lett., 1997. **79**(16): p. 3090.

101. Cui, Q. and I. Bahar, *Normal mode analysis: theory and applications to biological and chemical systems.* 2005: CRC press.

102. Yang, L., G. Song, and R.L. Jernigan, *Protein elastic network models and the ranges of cooperativity.* Proceedings of the National Academy of Sciences, 2009. **106**(30): p. 12347-12352.

103. Fuglebakk, E., S.P. Tiwari, and N. Reuter, *Comparing the intrinsic dynamics of multiple protein structures using elastic network models.* Bioch. Biophys. Acta, 2015. **1850**(5): p. 911-922.

104. Thorpe, M., *Comment on elastic network models and proteins.* Physical biology, 2007. **4**(1): p. 60.

105. Eyal, E. and I. Bahar, *Toward a molecular understanding of the anisotropic response of proteins to external forces: insights from elastic network models.* Biophys. J., 2008. **94**(9): p. 3424-3435.

106. Ikeguchi, M., et al., *Protein structural change upon ligand binding: linear response theory.* Phys. Rev. Lett., 2005. **94**(7): p. 078102.

107. Atilgan, C., et al., *Manipulation of conformational change in proteins by single-residue perturbations.* Biophys. J., 2010. **99**(3): p. 933-943.

108. Atilgan, C. and A.R. Atilgan, *Perturbation-response scanning reveals ligand entry-exit mechanisms of ferric binding protein.* PLoS Comput. Biol., 2009. **5**: p. e1000544.

109. Verkhivker, G.M., *Dynamics-based community analysis and perturbation response scanning of allosteric interaction networks in the TRAP1 chaperone structures dissect molecular linkage between conformational asymmetry and sequential ATP hydrolysis.* Bioch. Biophys. Acta 2018. **1866**(8): p. 899-912.

110. Zhang, S., et al., *Shared signature dynamics tempered by local fluctuations enables fold adaptability and specificity.* Molecular biology and evolution, 2019. **36**(9): p. 2053-2068.

111. Bakan, A., et al., *Evol and ProDy for bridging protein sequence evolution and structural dynamics.* Bioinformatics, 2014. **30**(18): p. 2681-2683.

112. Bakan, A., L.M. Meireles, and I. Bahar, *ProDy: protein dynamics inferred from theory and experiments.* Bioinformatics, 2011. **27**(11): p. 1575-1577.

113. Zilka, O., et al., *On the mechanism of cytoprotection by ferrostatin-1 and liproxstatin-1 and the role of lipid peroxidation in ferroptotic cell death.* ACS central science, 2017. **3**(3): p. 232-243.

114. Shah, R., M.S. Shchepinov, and D.A. Pratt, *Resolving the role of lipoxygenases in the initiation and execution of ferroptosis.* ACS Cent. Sci., 2018. **4**(3): p. 387-396.

115. Lamade, A.M., et al., *Inactivation of RIP3 kinase sensitizes to 15LOX/PEBP1-mediated ferroptotic death.* Redox Biol., 2022. **50**: p. 102232.

116. Jones, R. and L. Hall, *A 23 kDa protein from rat sperm plasma membranes shows sequence similarity and phospholipid binding properties to a bovine brain cytosolic protein.* Biochimica et Biophysica Acta (BBA)-Protein Structure and Molecular Enzymology, 1991. **1080**(1): p. 78-82.

117. Shemon, A.N., et al., *Characterization of the Raf kinase inhibitory protein (RKIP) binding pocket: NMR-based screening identifies small-molecule ligands.* PLoS One, 2010. **5**(5): p. e10479.

118. Atmanene, C., et al., *Characterization of human and bovine phosphatidylethanolamine-binding protein (PEBP/RKIP) interactions with morphine and morphine-glucuronides determined by noncovalent mass spectrometry.* Med. Sci. Monitor, 2009. **15**(7): p. BR178-BR187.

119. Noh, H.S., et al., *PEBP1, a RAF kinase inhibitory protein, negatively regulates starvation-induced autophagy by direct interaction with LC3.* Autophagy, 2016. **12**(11): p. 2183-2196.

120. Kuhn, H., M. Walther, and R.J. Kuban, *Mammalian arachidonate 15-lipoxygenases: structure, function, and biological implications.* Prostaglandins Other Lip. Mediat., 2002. **68**: p. 263-290.

121. Oliw, E.H., *Plant and fungal lipoxygenases.* Prostaglandins & other lipid mediators, 2002. **68**: p. 313-323.
122. Hansen, J., et al., *Bacterial lipoxygenases, a new subfamily of enzymes? A phylogenetic approach.* Applied Microbiol. Biotech., 2013. **97**(11): p. 4737-4747.
123. Horn, T., et al., *Evolutionary aspects of lipoxygenases and genetic diversity of human leukotriene signaling.* Progress in lipid research, 2015. **57**: p. 13-39.
124. Stover, C.K., et al., *Complete genome sequence of Pseudomonas aeruginosa PAO1, an opportunistic pathogen.* Nature, 2000. **406**(6799): p. 959-964.
125. Tacconelli, E., et al., *Discovery, research, and development of new antibiotics: the WHO priority list of antibiotic-resistant bacteria and tuberculosis.* Lancet Infect. Dis., 2018. **18**(3): p. 318-327.
126. De Boeck, K., *Cystic fibrosis in the year 2020: A disease with a new face.* Acta paediatrica, 2020. **109**(5): p. 893-899.
127. Finn, R.D., et al., *The Pfam protein families database: towards a more sustainable future.* Nucl. Aci. Res., 2015. **44**(D1): p. D279-D285.
128. Yang, L.-W. and I. Bahar, *Coupling between catalytic site and collective dynamics: a requirement for mechanochemical activity of enzymes.* Structure, 2005. **13**(6): p. 893-904.
129. Cinelli, M.A., et al., *Inducible nitric oxide synthase: Regulation, structure, and inhibition.* Medicinal research reviews, 2020. **40**(1): p. 158-189.
130. Lei, X., S.E. Barbour, and S. Ramanadham, *Group VIA Ca2+-independent phospholipase A2 (iPLA2β) and its role in β-cell programmed cell death.* Biochimie, 2010. **92**(6): p. 627-637.
131. Greenberg, M.E., et al., *The lipid whisker model of the structure of oxidized cell membranes.* Journal of Biological Chemistry, 2008. **283**(4): p. 2385-2396.
132. Zhang, S., et al., *ProDy 2.0: Increased Scale and Scope after 10 Years of Protein Dynamics Modelling with Python.* Bioinformatics, 2021.
133. Finn, R.D., et al., *The Pfam protein families database: towards a more sustainable future.* Nuc. Aci. Res., 2015. **44**(D1): p. D279-D285.
134. Rosenbaum, D.M., et al., *GPCR engineering yields high-resolution structural insights into β2-adrenergic receptor function.* Science, 2007. **318**(5854): p. 1266-1273.
135. Hanlon, C.D. and D.J. Andrew, *Outside-in signaling–a brief review of GPCR signaling with a focus on the Drosophila GPCR family.* J. Cell Sci., 2015. **128**(19): p. 3533-3542.

V. Presentation of significant scientific activity carried out at more than one university, scientific or cultural institution, especially at foreign institutions.

My scientific activity abroad was conducted at both American and European universities:

- Postdoctoral associate in the *School of Medicine* at the *University of Pittsburgh* (USA) in Prof. Ivet Bahar group for 30 months, from January 2016.

- *Assistant-doctorant* in the *Laboratory of Physics of Living Matter*, *École Polytechnique Fédérale de Lausanne* (EPFL) in Prof. Giovanni Dietler group for 6 months, from September 2013 (*during Ph.D. studies*).

This activity concerned research and articles that contribute to the achievement discussed in point IV.2.2 and parts of other research discussed in point IV.2.3.

I am collaborating with scientists from different universities (the US and Europe):
- Group of Prof. Valeriana Kagan, Department of Environmental and Occupational Health and Center for Free Radical and Antioxidant Health, University of Pittsburgh, Pittsburgh, USA.
- Group of Prof. Hülya Bayır, Department of Critical Care Medicine, Safar Center for Resuscitation Research, Children's Neuroscience Institute, Children's Hospital of Pittsburgh, University of Pittsburgh, Pittsburgh, USA.
- Prof. Ivet Bahar, Laufer Center for Physical and Quantitative Biology, Stony Brook University, New York, USA.

- Group of Patrick van der Wel, Zernike Institute for Advanced Materials, University of Groningen, Groningen, the Netherlands.
- Group of Prof. Sally Wenzel, Department of Medicine, University of Pittsburgh, Pittsburgh, PA, USA.
- Group of Prof. Andy VanDemark, Department of Biological Science, University of Pittsburgh, Pittsburgh, USA.
- Group of Prof. Moshe Arditi, Department of Biomedical Sciences and Department of Pediatrics, Cedars-Sinai Medical Center, Los Angeles, USA.
- Group of Prof. Bruno Lapied, Laboratoire Signalisation Fonctionnelle des Canaux Ioniques et des Récepteurs (SiFCIR), Université d'Anger, France.
- Dr. James M. Krieger, Polytechnic School at Universidad Autónoma de Madrid, Spain.

VI. Presentation of teaching and organizational achievements as well as achievements in the popularization of science.

VI.1. Didactics

In the past years, I was teaching the following subjects/classes:

Classes	Year
Mathematical analysis 1	2018/2019
Mathematical analysis 2	2018/2019
Basic programming 1	2018/2019
Basic programming 2	2018/2019
Introduction to Unix (exercises and lecture)	2018/2019 (2 groups)
	2015/2016 (2 groups)
Biopython computational course	2015/2016
Molecular Dynamics	2015/2016

Before obtaining the doctoral degree:

Classes	Year
Programming languages (C programming language)	2013/2014 (2 groups)
Symbolic systems (exercises and lecture)	2013/2014
Computer lab III – Unix and the Internet	2012/2013 (2 groups)
	2011/2012
	2010/2011
The physics of information processing (assisting in lecture)	2011/2012
Computer lab I – Basics of using computers	2010/2011
Molecular dynamics methods – Computer modeling of biomolecules	2009/2010
Elementary Physics (compensatory classes for 1st-year students)	2009/2010

Since October 2020, I have worked in a research position financed by the SONATA15 program from the Polish National Science Center, therefore, I do not conduct classes. Before that, I was a post-doc at the University of Pittsburgh, where I was not teaching. In the meantime had three breaks due to maternity leaves.

Several times I conducted scientific workshops in the field of biophysics/bioinformatics for participants (in English) of:
o Computational *Biophysics Workshop* organized by the members of the *Theoretical and Computational Biophysics Group* from the University of Illinois at Urbana-Champaign (UIUC) and the *National Center for Multiscale Modeling of Biological*

Systems (MMBioS) from the University of Pittsburgh, three times in 2016, 2017 and 2018 (Pittsburgh, USA).

o Conference *Bioinformatics in Torun (BIT) in 2010 and 2011. BIT is* organized by the Polish Bioinformatics Society (PTBI) and the Nicolaus Copernicus University in Torun, Poland.

o Summer Camp for International Students and Ph.D. Students in the program of the Polish National Agency for Academic Exchange SPINAKER – Intensive International Education Programs 12-14th July 2022 (Torun, Poland) – 2 groups, 3 hours each training.

Supervision of scientific works at NCU:

- o I am the assistant supervisor of the following doctoral students:
    - Thiliban Manivarma, MSc (since 2020, ongoing)
    - Beata Niklas, MSc (2018-2020)
- o I am a supervisor of master students:
    - Radosław Siwiński (since 2022, ongoing)
- o I am/was a supervisor of bachelor of engineering students:
    - Mateusz Czarnecki (since 2020, ongoing)
    - Mateusz Mnich (since 2020, ongoing)
    - Mariusz Konstanty (2022)

The lack of supervision for students before 2019 results from the 2.5-year postdoctoral fellowship until June 2018 and being on maternity leave (3 times after obtaining the doctoral degree: 2014/15, 2017/18, 2019/20).

VI.2. Organization

o Assistance in organizing, teaching international hands-on workshop: *Computational Biophysics Workshop at Pittsburgh* (2016-2018, 3 times, Pittsburgh, USA).

o Assistance in organizing and coordinating international conferences:
- *Bioinformatics in Torun* (Torun, Poland) organized by the Polish Bioinformatics Society (PTBI) and the Nicolaus Copernicus University in Torun, in the period 2009-2022 (6 times, 60-100 participants every year).
- *13th annual conference in bioinformatics* SocBiN (26-29 VI 2013, Torun, Poland).

o I was the president of the Faculty Doctoral Scholarship Committee FPAI NCU (2011-2013, *before the doctorate degree*).

VI.3. Popularization of science

I co-conducted lectures and workshops:

o Inaugural lecture for students of the Faculty of Physics, Astronomy and Informatics NCU (October 2015).

o Festival of Science and Art in Toruń ["Virtual journey inside the body – the exploration of biological nanostructures" (2009), "Secrets of fluorescence – where glowing rabbits come from (2010) and computer workshops "The beauty of molecular mechanisms of nature – how the biomechanics of the body works" (2011) and co-lecture "Luminous wonders of nature – secrets of protein fluorescence"].

- o Toruń Scientists' Night (lecture "OCT – human optical tomograph")
- o Before obtaining a doctoral degree, I also co-organized and participated in numerous popularizing campaigns, including conducting physical shows for hundreds of primary and secondary school students, including "Back to School" educational campaigns, Physics Demonstration Lessons implemented as part of the project Middle School Academy of Sciences for the subregion Koniński, Gymnasium Academy of Sciences, "Open your eyes, turn on your thinking", shows by the Polish Physical Society, etc.

More about the popularization of science can be found in section II.3 in the *List of scientific achievements*.

VII. Other relevant information.

I was on maternity and parental leave three times for 9-12 months with each kid (date of birth: X 2014, IX 2017, X 2019).

…………..……..……………….
(Applicant's signature)